*Review*

# Hydrogen Refueling Process: Theory, Modeling, and In-Force Applications

**Matteo Genovese** [1] , **Viviana Cigolotti** [2,*] , **Elio Jannelli** [3] **and Petronilla Fragiacomo** [1]

1   Department of Mechanical, Energy and Management Engineering, University of Calabria, Arcavacata di Rende, 87036 Cosenza, Italy
2   Laboratory for Energy Storage, Batteries and Hydrogen Production and Utilization Technologies, Department of Energy Technologies and Renewable Sources, ENEA—Italian National Agency for New Technologies, Energy and Sustainable Economic Development, Research Centre of Portici, 80055 Naples, Italy
3   Department of Engineering, University of Naples "Parthenope", Centro Direzionale Is. C4, 80143 Naples, Italy
*   Correspondence: viviana.cigolotti@enea.it; Tel.: +39-347-686-1412

**Abstract:** Among the alternative fuels enabling the energy transition, hydrogen-based transportation is a sustainable and efficient choice. It finds application both in light-duty and heavy-duty mobility. However, hydrogen gas has unique qualities that must be taken into account when employed in such vehicles: high-pressure levels up to 900 bar, storage in composite tanks with a temperature limit of 85 °C, and a negative Joule–Thomson coefficient throughout a wide range of operational parameters. Moreover, to perform a refueling procedure that is closer to the driver's expectations, a fast process that requires pre-cooling the gas to −40 °C is necessary. The purpose of this work is to examine the major phenomena that occur during the hydrogen refueling process by analyzing the relevant theory and existing modeling methodologies.

**Keywords:** hydrogen refueling process; hydrogen station; review; vehicle filling; storage cascading; hydrogen pre-cooling; Joule–Thomson; pressure regulator

## 1. Introduction

Hydrogen technologies are recognized worldwide as efficient and effective decarbonizing solutions [1,2]. Their application has been widely demonstrated in several energy sectors, such as in fuel cell systems for stationary applications [3], intensive industrial applications [4], and sustainable mobility [5,6].

Regarding the latter, hydrogen fuel cell electric vehicles (FCVs) are deployed in several countries, being previously tested as prototypes by different automakers, and in several applications: material handling vehicles [7,8], urban light-duty vehicles [9], sedan and SUVs [10,11], heavy-duty trucks [12–14], and even trains [15,16]. Samsun et al. [17] recently presented the current state-of-art deployment of such vehicles, with a focus on several countries and their strategic plans and vision for 2030 and 2050. In Europe, in 2021, there were about 3960 FCVs, while in North America and Asia there were 12,600 and 34,600 [18], respectively.

The main infrastructures supporting this new mobility are the so-called hydrogen refueling stations (HRS), which are facilities designated to dispense hydrogen from on-site storage systems to vehicle tanks [19]. In Europe, the Alternative Fuels Infrastructure Regulation (AFIR) has recently stipulated that there must be "one hydrogen refueling station (HRS) every 100 km along the Ten-T core and full networks, with a daily capacity of at least 2 tonnes and a minimum 700 bar dispenser at each station" [20]. By the end of 2027, a minimum number of stations must be installed. It was also determined that liquid HRSs would be constructed every 400 km and that there would be at least one HRS for each urban node, a functional area consisting of one or more central cities and the rural

regions around them [20]. In addition, by 2027, data access hubs for alternative fuels will be built to offer information about HRS availability, lead times, and pricing discrepancies.

The process of dispensing hydrogen is complex, and it must take into account conditions for a "customer acceptable experience" [21,22], close to requirements of conventional vehicles, such as diesel and gasoline, such as:

- Acceptable charging times necessary to guarantee a full tank;
- Driving range of more than 500 km;
- Fossil parity, or technical and economic goals equivalent to those of the corresponding technologies based on fossil fuels (e.g., diesel), in order to encourage the adoption of hydrogen technology.

The corresponding technical requirements in the process of dispensing hydrogen are challenging. Given the non-liquid nature of hydrogen stored in the vehicle, it is significantly more difficult to describe the amount of hydrogen required for a "full tank" with the former criterion. Such a characteristic is required to determine when a vehicle's fuel tank may be regarded as full, and refilling can be declared complete. However, the density fluctuates with pressure and temperature. Moreover, during the refilling process, compression generates heat within the fuel tank. Currently, available FCV tanks are designed to function between $-40$ and $85\ °C$ [23]. In addition to providing significant safety risks for the vehicle and station [24,25], the increase in temperature affects the tank's filling level; at the same pressure, the higher the temperature, the less dense the gas.

For this reason, an ideal fueling strategy strives to swiftly fill all hydrogen storage systems to a high state of charge (SOC), never exceeding the storage system operational limitations of $85\ °C$ for the internal tank, without overheating and without overfilling (SOC more than 100%) [26]. Moreover, such a procedure must direct hydrogen refueling within an acceptable duration without exceeding the temperature and pressure restrictions, as well as maximum pressure levels, to obtain a suitable SOC, between 90% and 100%, under varying ambient temperatures [27,28].

In terms of the number of FCEVs and HRSs now on the road, three nations—the United States, Germany, and Japan—dominate the global market [29,30]. Unsurprisingly, several nations now have significant producers of HRS essential components and systems. Using bottom-up cost analysis, Mayyas et al. [31] evaluated the industrial competitiveness of the area. The objectives were to analyze the competitiveness of American manufacturers in comparison to other nations and to better understand the primary manufacturing cost factors in each of the target countries. The bottom-up cost study for the key systems in hydrogen stations showed that American manufacturers benefit from greater expertise, cheaper energy, and reduced transportation costs when equipment is delivered inside the U.S. mainland.

Even though the complexity of the process is clear, to the best knowledge of the authors, there is no comprehensive state of the art and review in the literature, highlighting in detail the phenomena and the technical and practical aspects of each area of a hydrogen refueling process (HRP).

Most of the papers, as discussed in the Material and Methods section, are focused on specific aspects of the HRP, e.g., modeling the temperature increase in the vehicle tank, monitoring the 3D temperature map within the vehicle tank, analyzing the achievable SOC under specific conditions, optimizing the pressure storage levels, but there is no comprehensive overview and review of all the different aspects inherent in an HRS operation during HRPs.

The present paper aims to present a comprehensive and comparable awareness of the current state of HRPs and their general approaches and technical challenges. As a result, the study can become a solid base for further improvements and investigations, presenting the related knowledge in a unique position to define and excel in the investigation and analysis of high-performance HRPs and the related HRS.

## 2. Materials and Methods

The two most important worldwide scientific databases, Web of Science (WoS) and Scopus, were examined in the literature analyses.

The keywords listed in Table 1 were then entered to conduct a search of the primary scientific contributions. The major findings of the bibliographic survey are shown in Figure 1. In contrast to the approximately 244 articles found on Scopus, around 548 articles were found on WoS between 1983 and 2023. The main distinction is related to the various kinds of study that both databases conducted. While Scopus searches for the desired terms simultaneously in the title, abstract, and keywords, WoS looks for articles that include the desired words in the title, abstract, or keywords.

**Table 1.** Literature Review Search Inputs and Results.

| Database | Search | Results |
|---|---|---|
| WoS | ((TI = ((hydrogen AND (refuelling OR refueling OR fueling OR fuelling) AND station AND (modelling OR modeling OR experimental)))) OR AB = ((hydrogen AND (refuelling OR refueling OR fueling OR fuelling) AND station AND (modelling OR modeling OR experimental)))) OR AK = ((hydrogen AND (refuelling OR refueling OR fueling OR fuelling) AND station AND (modelling OR modeling OR experimental))) | 548 |
| Scopus | (TITLE-ABS-KEY (hydrogen AND (refuelling OR refueling OR fueling OR fuelling) AND station AND (modelling OR modeling OR experimental))) | 244 |
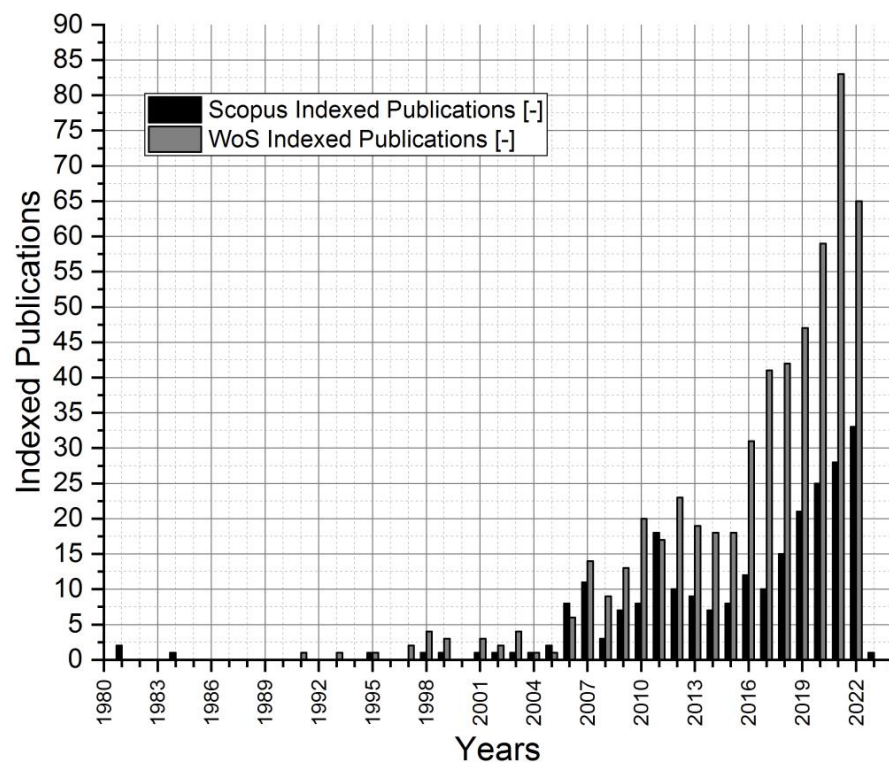


**Figure 1.** Literature Review on WoS and Scopus.

It is possible to see with interest how scientific activities have significantly increased in recent years. Genovese and Fragiacomo [19] recently performed a literature assessment of the most current research efforts related to HRS, noting new trends about the various components involved in HRS functioning and tracing the primary layouts of this infrastructure.

In light of current research on relevant keywords, the most active research institutions in the HRS area as well as international collaborations were examined. The primary collaborations were recognized by the use of VOSviewer [32,33], as shown in Figure 2a,b, respectively, by cooperation intensity and most recent activities, by processing the Scopus dataset.
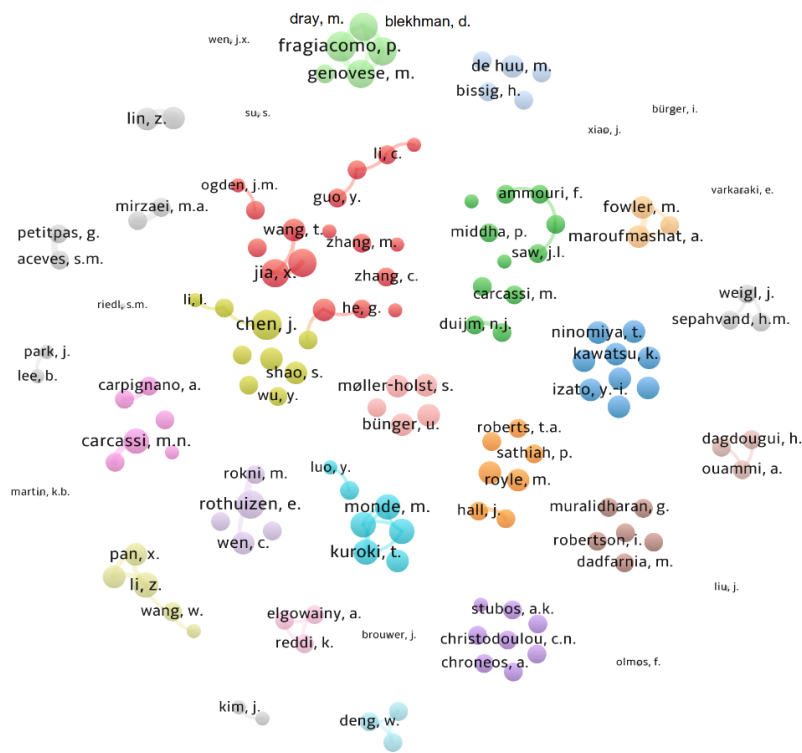
(**a**)
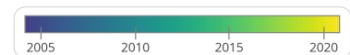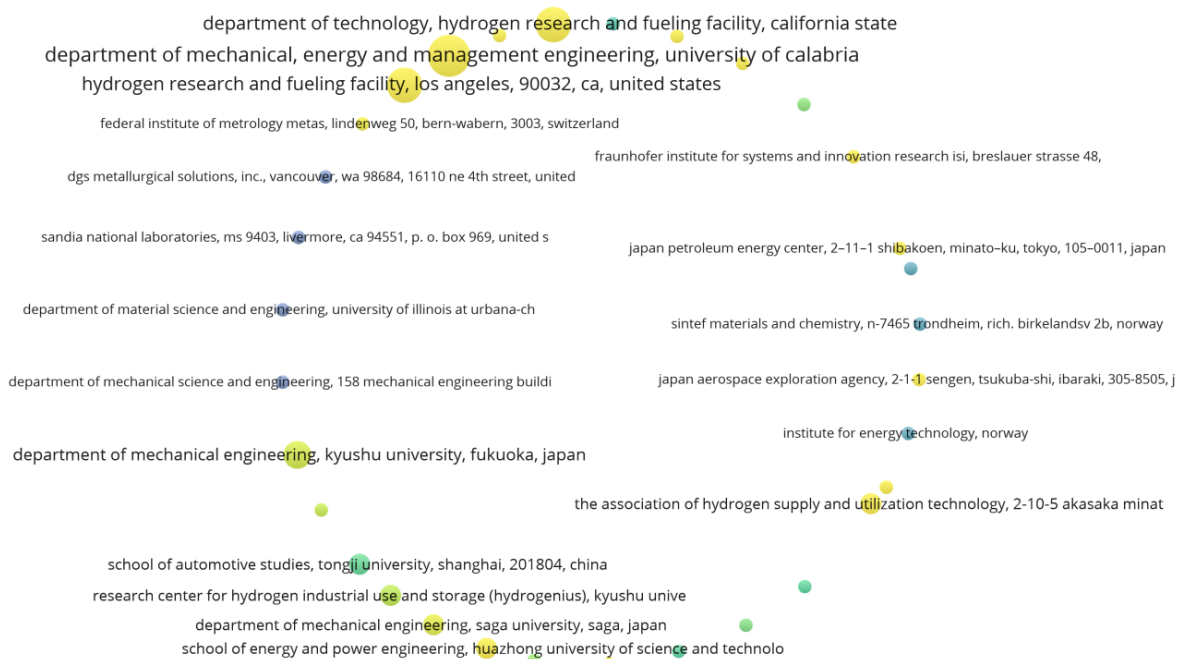


(**b**)
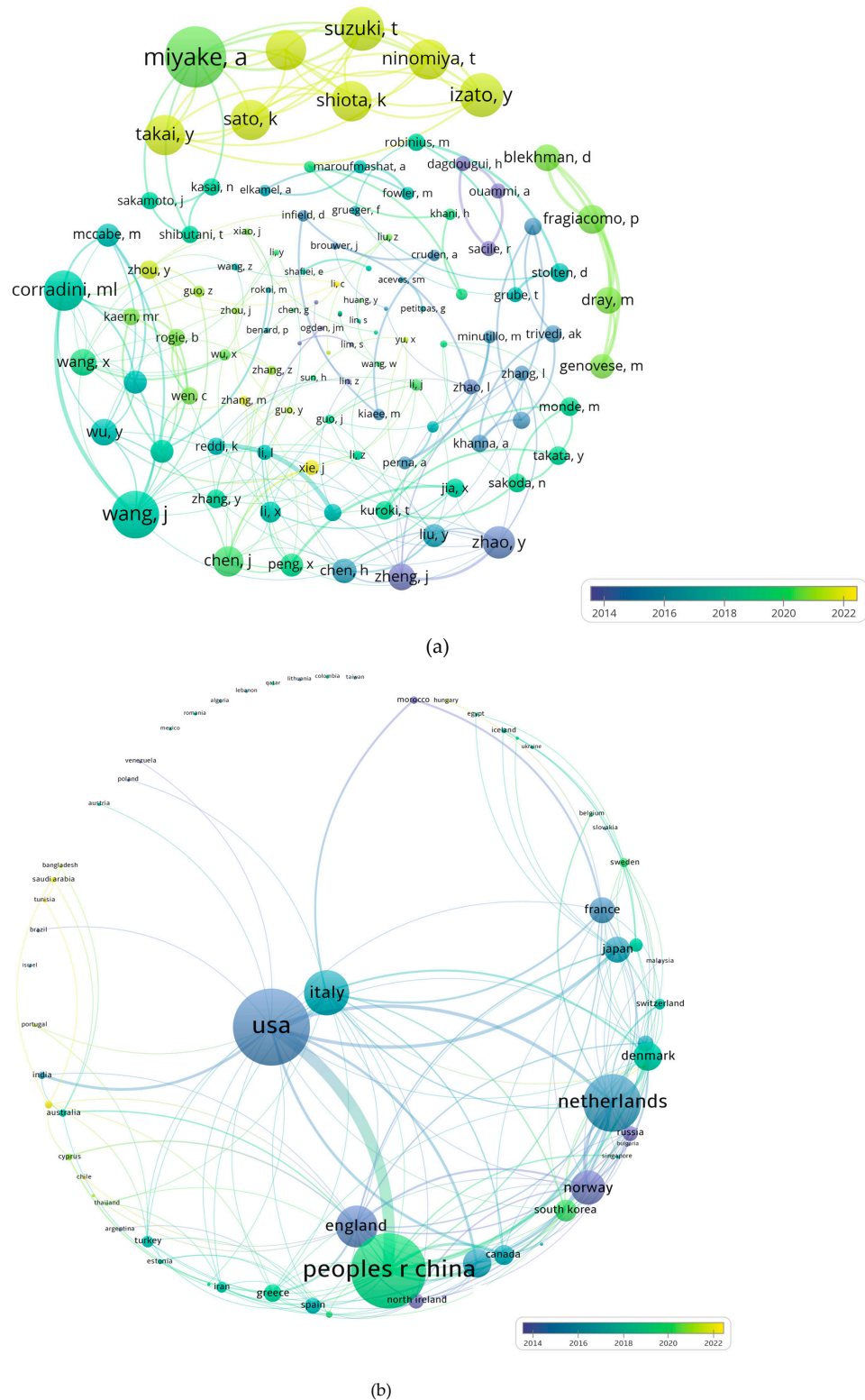
**Figure 2.** Clusters of authors according to VOSviewer (**a**) and Organizations' collaborations (**b**), by processing Scopus database.

The Fuel Cell and Hydrogen Research Team, at the Department of Mechanical, Energy, and Management Engineering, has the most active authors worldwide on this topic, according to the Scopus database, with a strong collaboration with the Hydrogen Research

and Fueling Facility, in Los Angeles, with the highest total link strength, according to VOSViewer. The Technical University of Denmark has the highest number of cumulated publications in Scopus, followed by Xi'an Jiaotong University, HSE Science and Research Centre, and Kyushu University. Authors' collaborations are shown in Figure 3a, according to the WoS database, while the country collaborations are presented in Figure 3b.



(a)



(b)

**Figure 3.** Clusters of authors according to VoSviewer (**a**) and Countries' collaborations (**b**), by processing WOS database.

The research organizations that have specialized in certain sectors of the HRS, including storage, dispensing lines, pressure regulators, pre-cooling, vehicle filling processes, and refueling procedures, have been identified via the literature study carried out for this work. As a result, the paper has been separated into six sections, where the most current research activities for each subject area will be given, with an emphasis on both the theory guiding the study and the innovations offered by the numerous research groups examined.

## 3. Refueling Process

This section aims to describe the theory and modeling of the main phenomena that occur during a hydrogen refueling process (HRP). The HRP considered configuration is shown in Figure 4. Hydrogen is retrieved from the HRS main storage system, to be cascaded to the vehicle tank. If the pressure level within the HRS main storage system is lower than the pressure level of the vehicle compressed hydrogen storage system (CHSS), a compressor is needed to achieve the refueling nominal pressure. Before entering the CHSS, hydrogen is cooled down via a hydrogen pre-cooling unit, to avoid the CHSS overheating. The pressure is controlled via the pressure control valve (PCV), which determines the pressure ramp rate and consequently the mass flow rate that is delivered to the vehicle tank.
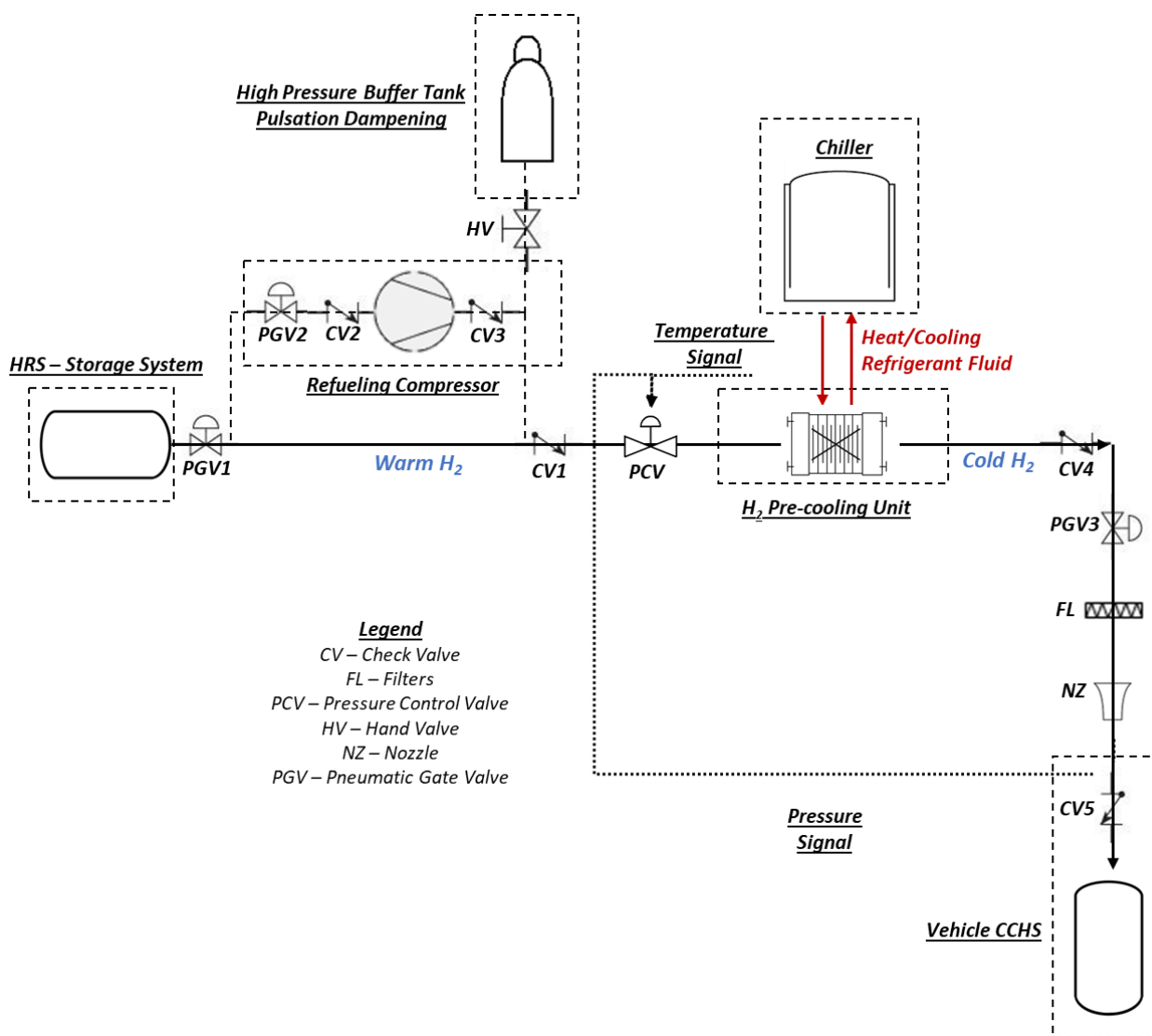


**Figure 4.** Concept of a schematized hydrogen refueling process.

### 3.1. Hydrogen Cascading

Hydrogen is normally stored at high pressure in an HRS. It can be produced on-site, via water electrolysis, at low pressure (up to 30–60 bar), and then compressed with a dedicated storage compression system [34,35], at a pressure of 450 bar, and even higher (900 bar). Another option is that it can be supplied via external tube trailers, already pressurized [36,37].

There are several typed of hydrogen tanks that can be used for compressed hydrogen, as shown in Figure 5. Existing hydrogen storage applications mostly employ categories III and IV [38,39]. These uses are distinct from storage applications in compressed natural gas vehicles, which typically utilize type I and II with natural gas compressed to 20–25 MPa. Based on type IV carbon-composite technology, hydrogen tank systems can store 350 bar and 700 bar compressed hydrogen.



**Figure 5.** Compressed Hydrogen, Storage Tanks.

Once hydrogen is drawn from the main storage tanks, according to Equation (1), the hydrogen density and consequently the pressure level of the storage system decrease.

$$m_{tank} = m_{tank,t_0} - \int_{t_0}^{t_0 + \Delta t} \dot{m}_{vehicle} \cdot dt \tag{1}$$

Given the high pressure characterizing the operating conditions of an HRP, ideal gas law is not satisfactory to realistically represent the physical and thermodynamic connection between temperature, pressure, and density. Real gas equations must be adopted, or data must be retrieved by a database with reliable sources and validation, as shown in Figure 6. Equation (2) represents a polynomial expression of hydrogen density as a function of hydrogen pressure and temperature, based on data plotted in Figure 7.

$$\rho_{H_2} = f\left(p_{H_2}, T_{H_2}\right) = a_{00} + a_{10} \cdot p + a_{01} \cdot T + a_{20} \cdot p^2 + a_{11} \cdot p \cdot T + a_{02} \cdot T^2 + a_{30} \cdot p^3 + a_{21} \cdot p^2 \cdot T + a_{12} \cdot p \cdot T^2 + a_{03} \cdot T^3 \tag{2}$$

To better manage hydrogen storage pressure levels, different authors investigated how they can affect the operation and the performance of an HRP. Table 2 lists the main contributions present in the literature, dealing with HRP and hydrogen storage tanks research-related activities. Most of the research efforts are focused on determining the best configuration for the cascade hydrogen storage systems, minimizing the energy expenditure of the HRP or the irreversibilities.
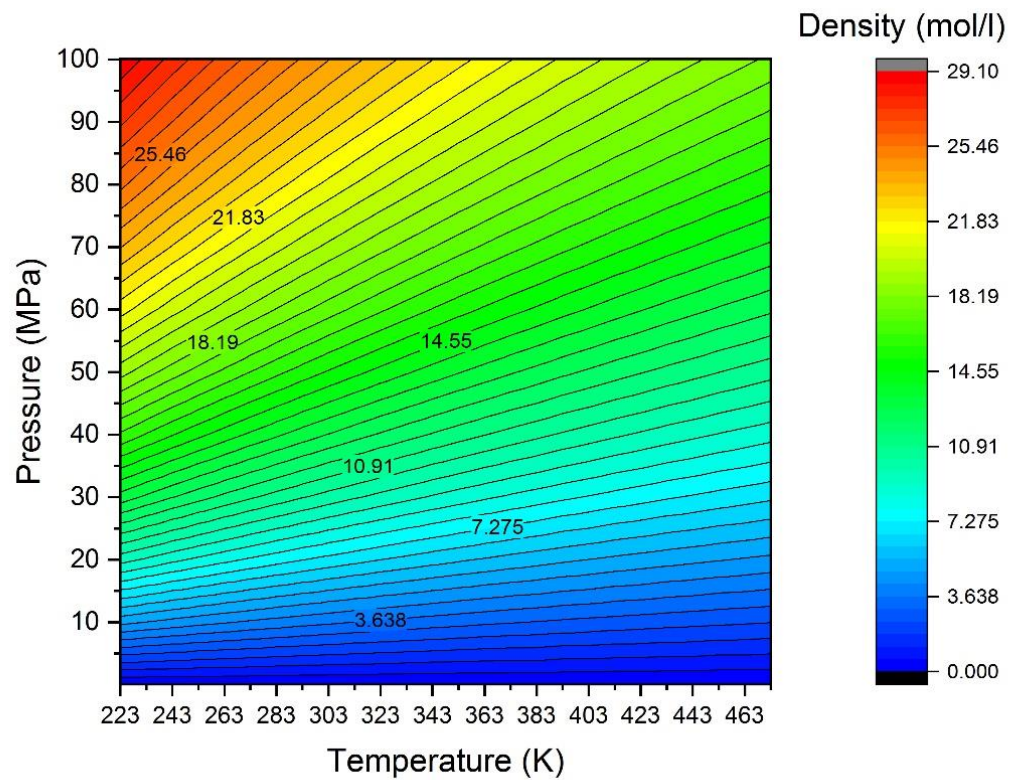
**Figure 6.** Hydrogen density levels as a function of pressure and temperature. Data processed from [40].
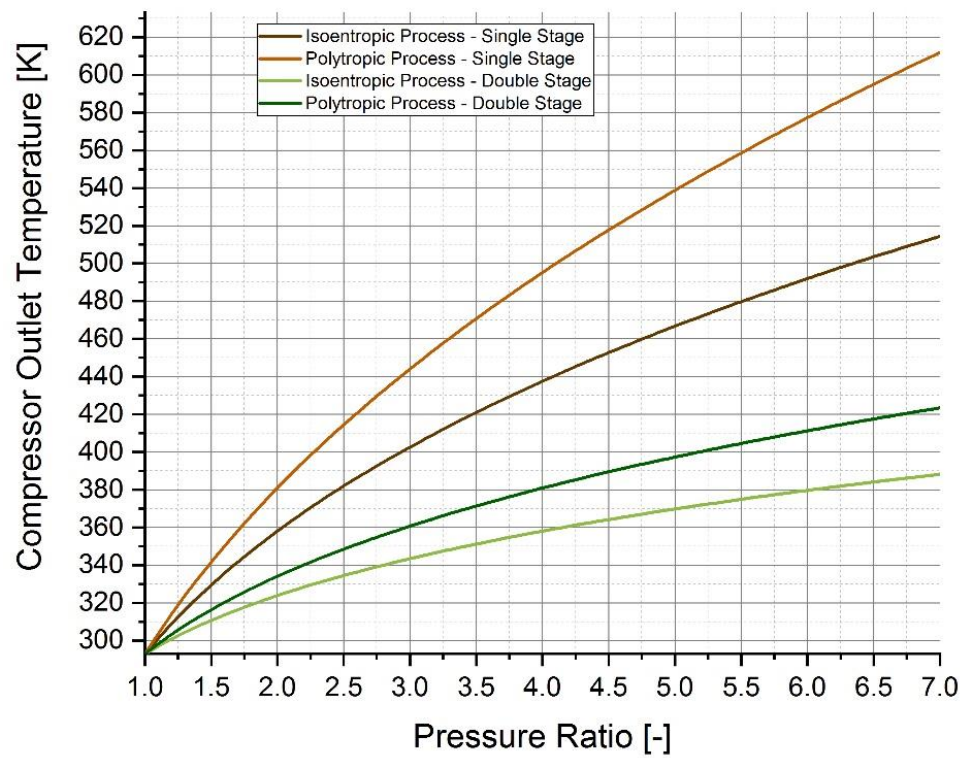


**Figure 7.** Hydrogen density levels as a function of pressure and temperature.

**Table 2.** Main research activities on cascade hydrogen storage.

| Authors | Year | Main Finding |
|---|---|---|
| Farzaneh-Gord et al. [41] | 2012 | A single pressure-level storage system requires around 66% less time than the cascade storage system to raise the vehicle CHSS to an ultimate pressure of 35 MPa but has higher entropy generation and therefore higher irreversibilities. |
| Rothuizen and Rokni [42] | 2014 | Cascading from three/four tanks with different pressure levels can reduce HRP energy consumption. |
| Elgowainy et al. [43] | 2014 | The compression cost at an HRS may be cut by approximately 60%, and the station's original capital expenditure can be reduced by around 40%, thanks to a consolidation method for a high-pressure (250-bar) tube-trailer. |
| Reddi et al. [44] | 2014 | The cost of refueling may also be decreased by lowering the tube trailer cut-off pressure for first vehicle refueling and raising the trailer's return pressure, particularly in early markets when the refueling stations will be greatly underused. |
| Sakoda et al. [45] | 2016 | Analysis on the dynamic temperature and pressure levels of high-pressure hydrogen at 100 MPa in a 1-L tank that is released via 0.1-mm- and 0.2-mm-diameter orifices that resemble fractures. |
| Talpacci et al. [46] | 2018 | At ambient temperature, a ratio of 0.12 between low-pressure and high-pressure buffer tanks guarantees the optimal configuration for low energy consumption at the hydrogen chiller. |
| Reddi et al. [47] | 2018 | Thanks to the development of two-tier "pressure consolidation" of supplied tube-trailers (or comparable supply storage), the throughput at HRSs has been increased. |
| Sadi and Deymi-Dashtebayaz [48] | 2019 | A comparison of buffer and cascade storage banks revealed that employing a buffer storage bank results in a 200-s reduction in refueling time. However, the buffer storage system has a larger energy need for gas storage. |
| Kawano et al. [49] | 2019 | Experimental and numerical analyses have been used to examine the heat transfer properties and vessel state changes that occur during the discharge phase. |
| Rogié et al. [50] | 2021 | Application of ejectors that replace expansion valves in HPR. |
| Xiao et al. [51] | 2021 | Operation with three storage systems allows an energy consumption reduction of 34%. |
| Xiao et al. [52] | 2021 | The research demonstrates that an on-board storage tank may be successfully refueled using a cascade filling method with a constant average pressure ramp rate (APRR), which may successfully minimize energy consumption by roughly 2.5% for charging periods under 183 s. |
| Yu et al. [53] | 2022 | The best volume ratio for a stationary storage capacity of 150 kg is 4-3-3, while that for a stationary storage capacity of 600 kg is 1-5-4. |
| Luo et al. [54] | 2022 | Choosing the correct starting pressure and capacity of cascade storage tanks may minimize cooling energy usage by up to 11%. |
| Caponi et al. [55] | 2022 | 10% less energy is needed for compression if a cascade procedure is applied. |
| Xu et al. [56] | 2022 | By alternating between the three banks in the sequence of decreasing pressure, a unique control mechanism for cascade replenishment was established. The findings suggest that this approach increases the daily refueling capacity of HRS by 5%. |

During the dynamic operation of an HRP, if the pressure level of the main tanks is lower than or approximately close to the pressure level within the CHSS, the station control operates the hydrogen compressor. In a hydrogen fuel station, a compressor is used to compress the hydrogen gas to high pressure for storage and dispensing. The compressor used in hydrogen fuel stations can be either a positive displacement compressor or a dynamic compressor [57,58]. Positive displacement compressors, such as reciprocating compressors, are commonly used in hydrogen fuel stations, as they are efficient and reliable at high pressures [59–61].

Compressors used in hydrogen fuel stations must be specially designed to handle the unique properties of hydrogen gas, including its low density, high flammability, and tendency to leak [62–64]. They are typically equipped with safety features such as pressure relief valves, and explosion-proof enclosures. Ligen et al. [65] used MATLAB to create a performance-predicting engineering tool for air-driven boosters in HRS. With an accuracy of 5%, it enables the user to mimic the process trends. Data on time, temperature, compression

cycles, and air consumption may be utilized for process management and maintenance planning in the context of a hydrogen refueling station.

When hydrogen is compressed, its outlet temperature can dramatically increase, due to the heat of compression. Equation (3) is an example of a polytropic relationship between inlet and outlet flows of a compression stage. Figure 7 depicts how the hydrogen outlet temperature can increase as a function of a compression stage, for different scenarios, such as a single-stage compression, both polytropic or isentropic, and a double-stage compression with an ideal inter-stage cooling. The hypothesis and the boundary conditions are listed in Table 3 As can be seen from Figure 7, for a pressure ratio of 7, the temperature can rise to 600 K for a single stage.

$$T_{outlet} = T_{outlet} \cdot \left( \frac{p_{outlet}}{p_{inlet}} \right)^{\frac{n-1}{n}} \tag{3}$$

**Table 3.** Hydrogen Compression Boundary Conditions.

| Parameter | Value |
|---|---|
| Isentropic Coefficient, $\gamma$ [-] | 1.407 [66] |
| Polytropic Coefficient, n [-] | 1.609 [67] |
| Initial Temperature [K] | 293 |
| Maximum Pressure Ratio [-] | 7 |

To approach this issue, some authors investigated how to mitigate the hydrogen temperature in a refueling process with an operating compressor. Genovese et. al. [68] analyzed how the output temperature may still easily exceed 50 °C, which has an impact on both the temperature of the dispenser hose and the energy consumption of the hydrogen chiller. After lowering the booster closed-loop water cooling temperature from 15 °C to 10 °C, the experimental effort aimed to represent a reduced energy demand for the booster and hydrogen chiller by lowering the temperature levels in the hose and at the booster output.

*3.2. Hydrogen Dispensing Line*

The HRP dispensing line is characterized by valves, joints, the required instruments of measurement [69–73] and the needed safety equipment [74–77]. Pressure losses can be calculated with Equation (4), where $k_v$ is a coefficient that accounts for length, diameter, and friction losses.

$$\Delta p = k_v \cdot \frac{1}{2} \cdot \rho \cdot v^2 \tag{4}$$

The heat exchanged with the environment is another important parameter to monitor the temperature level evolution across the pipes, which affects the final temperature at the hose and therefore the inlet temperature at the vehicle tank. Equation (5) could be used to evaluate the temperature evolution, by including the active area for thermal dissipation A, the heat coefficient h, and the temperature delta between the hydrogen flow and the external temperature. Table 4 lists the range of thermal mass values for the main components in the dispensing line, namely pipes, hoses, nozzle, and breakaway.

$$Q_{loss} = A \cdot h \cdot \left( T_{H_2} - T_\infty \right) \tag{5}$$

**Table 4.** Thermal Mass of several components in the dispensing line. Data retrieved from [78].

| Component | Thermal Mass [kJ/kg] |
|---|---|
| Pipe | 0.56–1.64 |
| Hose, Nozzle and Breakaway | 2.71–3.14 |

Among other components in the dispensing line, an extra high-pressure buffer capacity is required when a retail hydrogen station uses booster compressors to directly fill automobiles in order to reduce the possibility of pressure pulsations in the system. Of no buffer capacity during 70 MPa fueling, pulsations with a magnitude up to 6.7 MPa were seen at the Cal State LA hydrogen fueling station, as shown in Figure 8.
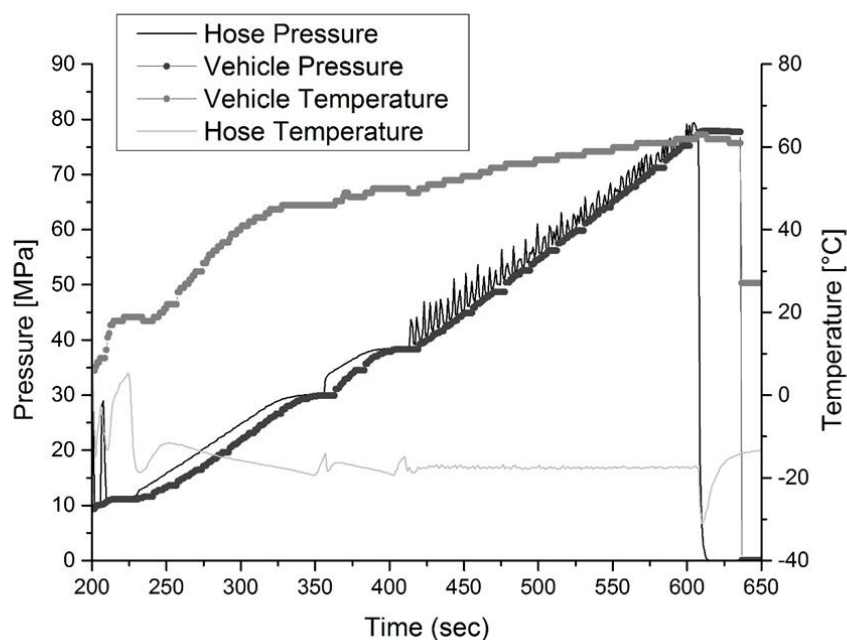


**Figure 8.** Pulsations on refueling processes with an operating compressor and without a buffer tank. Reproduced with permission from [78], Elsevier, 2023.

Therefore, the emphasis was on figuring out the minimal buffer volume needed to assure that the whole downstream system would operate without pulsations (booster compressors, piping, and the vehicle hydrogen hardware). The authors found that a tank with a capacity of 0.05 m$^3$ can keep the station's pressure pulsation below 0.2 MPa, ensuring the station's good functioning [79].

The steps below are typically used to fill a fuel cell vehicle's hydrogen storage system:

1. Joining the hydrogen fueling station's dispenser to the fuel cell vehicle.
2. Pumping up the dispenser's pressure to the desired level, usually around 700 bar.
3. Allowing the hydrogen to flow from the dispenser into the storage system by opening the fuel cell vehicle's fill valve.
4. Controlling the filling process to check for leaks or other issues and to ensure that the storage system is being filled to the proper pressure level.
5. After the storage system is full, shutting off the fuel cell vehicle's fill valve.
6. Cutting the vehicle's connection to the dispenser and looking for leaks.

Genovese et al. [80] analyzed hydrogen losses during the stand-by period and the dynamic operation of HRSs. While possible losses during the station's regular operation should be taken into account, leaks during the station's standby time may be disregarded. The most important tasks are those related to maintenance, and regular checklists may be carried out to reduce leaks or stop failures and leaks. The authors advised closing the manual valve on the low-pressure buffer tank when the dispenser is restarted because every time this step is skipped, 0.5 kg of hydrogen could escape and vent.

Other important types of equipment are the safety valves, which are essential in preventing ruptures during HRS operation [81–83]. The mass flow vented by the system is a function of the pressure within the pipe and the ambient pressure, and it also depends on the Mach number. The hydrogen speed of sound is higher compared to other gases, and its value is depicted in Figure 9 as a function of pressure and temperature. Equation (6)

can be adopted to evaluate the vented mass flow in subsonic and supersonic regimes. Zou et al. [84] approached the leakage analysis from high-pressure tanks and proposed a new formula to calculate the flow rate. After analyzing and contrasting several gas state equations and enthalpy formulae, a high-pressure gas leakage process model with heat exchange corrections (HEC model) was established. Results indicated that when compared to earlier models, the suggested model is more likely to provide accurate predictions of the mass flow rate, pressure, and temperature of gases that leak within hydrogen storage devices.

$$
\dot{m} = \begin{cases} C_v \cdot \frac{\pi \cdot d^2}{4} \cdot \sqrt{2 \cdot \rho_1 \cdot p_1 \cdot \frac{\gamma}{\gamma-1} \cdot \left[ \left( \frac{p_2}{p_1} \right)^{\frac{2}{\gamma}} - \left( \frac{p_2}{p_1} \right)^{\frac{\gamma+1}{\gamma}} \right]} \; if \; \frac{p_2}{p_1} > \left( \frac{2}{\gamma+1} \right)^{\frac{\gamma}{\gamma-1}} \\[20pt] C_v \cdot \frac{\pi \cdot d^2}{4} \cdot \sqrt{2 \cdot \rho_1 \cdot p_1 \cdot \frac{\gamma}{\gamma+1} \cdot \left[ \left( \frac{2}{\gamma+1} \right)^{\frac{2}{\gamma-1}} \right]} \; if \; \frac{p_2}{p_1} \le \left( \frac{2}{\gamma+1} \right)^{\frac{\gamma}{\gamma-1}} \end{cases}
\tag{6}
$$
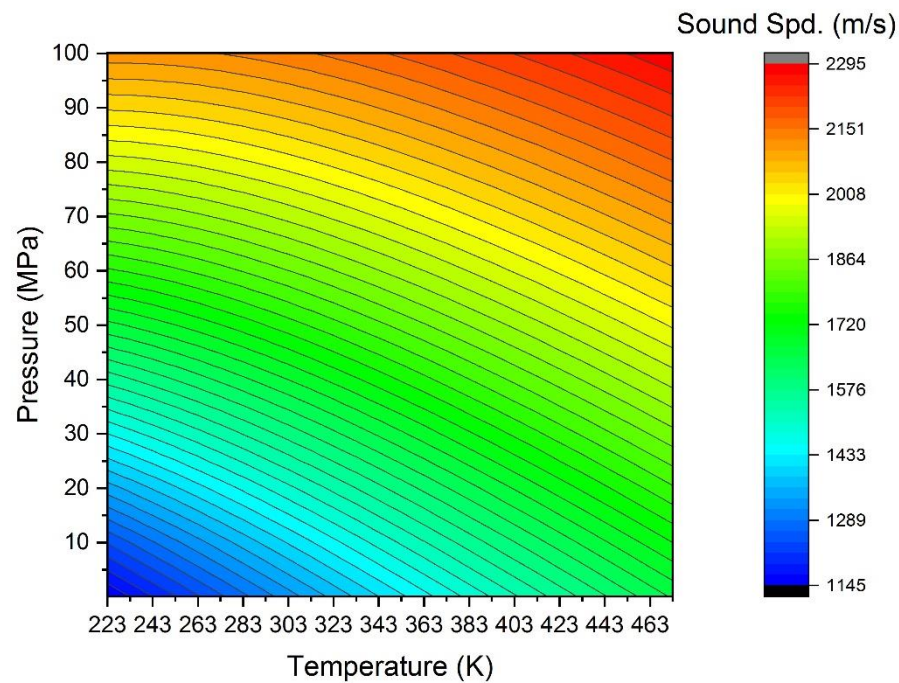


**Figure 9.** Hydrogen speed of sound as a function of pressure and temperature. Data processed from [40].

### 3.3. Hydrogen Pressure Regulator

In a fuel station or other application, a hydrogen pressure regulator is a device that manages the pressure of hydrogen gas. For storage or dispensing, the pressure regulator lowers the pressure of the compressed hydrogen coming from the compressor to the desired level. It operates by modifying the gas flow through a valve or orifice that regulates the pressure. A specific pressure, such as 700 bar for storage or 350 bar for dispensing, is typically set on the regulator. The low density, high flammability, and propensity for leakage of hydrogen gas are just a few of the characteristics of hydrogen gas that hydrogen pressure regulators are made to accommodate. Safety features such as pressure relief valves and explosion-proof enclosures are frequently included in them.

When a gas is cooled or expanded, the Joule–Thomson (J–T) effect, takes place. The temperature and internal energy of a gas change when it is cooled or expanded. The shift

in temperature that takes place as a result of this internal energy change is known as the Joule–Thomson effect, described by Equation (7).

$$\mu_{JT} = \left(\frac{\partial T}{\partial p}\right)_h \quad when \quad h_{in}(T_{in}, p_{in}) = h_{out}(T_{out}, p_{out}) \tag{7}$$

As shown in Figure 10, the Joule–Thomson coefficient for hydrogen is negative, indicating that when hydrogen is expanded at constant enthalpy, the temperature will raise.
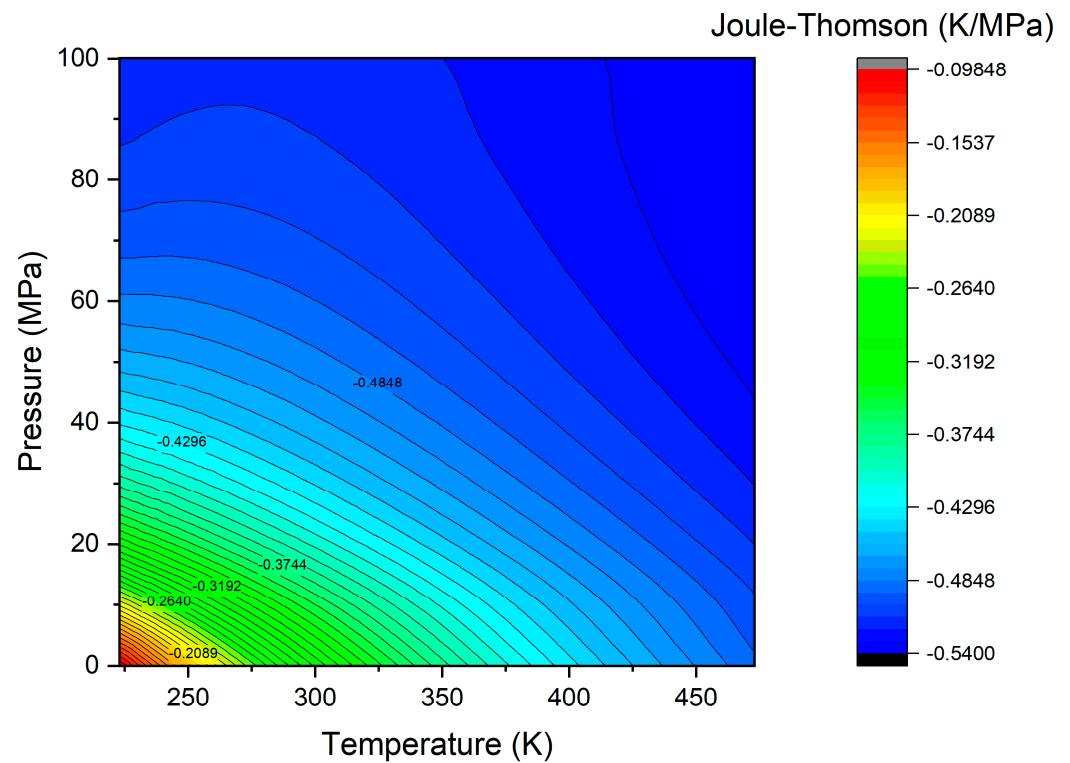


**Figure 10.** Joule-Thomson coefficient values for several pressure and temperature levels. Data processed from [40].

This effect is applied in the pressure regulator valves in HRSs, identified as Joule–Thomson expansion valves, which expand hydrogen gas. The temperature increases as a result of the expansion, affecting the final temperature at the hose and therefore the inlet temperature at the vehicle tank. During a refueling process, the required pressure level at the hose is established by the definition of an Average Pressure Ramp Rate (APRR) [85]. Therefore, the mass flow passing through the pressure regulator and dispensed to the vehicle can be calculated by employing Equation (8).

$$m_{H_2} = \sqrt{\frac{\Delta p \cdot \rho}{C_v}} = \sqrt{\frac{(p_{storage} - p_{APRR}) \cdot \rho}{C_v}} \tag{8}$$

Moreover, Li et al. [86] investigated how the Joule–Thomson effect of high-pressure hydrogen in a pressure regulator valve may generate substantial temperature variations. Low pressure negates the Joule–Thomson effect's temperature reduction. The authors, therefore, found a correlation for calculating the Joule–Thomson coefficient as a function of the compressibility factor Z and of the specific heat at constant pressure.

$$\mu_{JT} = \frac{1}{c_p}\left[T\left(\frac{\partial V}{\partial T}\right)_p - V\right] = \frac{R \cdot T^2}{p \cdot c_p}\left(\frac{\partial Z}{\partial T}\right)_p \tag{9}$$

*3.4. Hydrogen Pre-Cooling*

In the operation of a hydrogen fuel station, cooling is necessary to keep the hydrogen at a low temperature and high pressure for storage and dispensing. This is typically done using a refrigeration system, which cools the hydrogen gas to around −40 °C [87]. A refrigerant is typically used in the refrigeration system to absorb heat from the hydrogen and transfer it to a different cooling system. The following is the fundamental procedure for cooling hydrogen in a fueling station:

1. The compressed hydrogen first travels through a heat exchanger.
2. The hydrogen cools as a result of the refrigerant absorbing heat from it.
3. A compressor is used to increase the refrigerant's pressure and temperature.
4. After passing through a condenser, the heated refrigerant releases its heat to the surrounding air or water.
5. To lower its pressure and temperature, the refrigerant is then passed through an expansion valve.
6. The process is then repeated with the refrigerant passing once more through the heat exchanger to pick up more heat from the hydrogen.

The cooled hydrogen is then kept at a high pressure of 700 bar and −40 °C and dispensed to the vehicle's tank. To ensure the station and vehicle's safety, it is crucial to note that the cooling system must be designed, produced, and tested in accordance with safety regulations and standards. Several factors, including coefficient of performance (COP), and energy consumption, can be used to evaluate the energy performance of a hydrogen precooling system in a hydrogen fueling station [88]. Elgowainy et al. [89] proposed the following correlation for calculating the COP of the hydrogen chiller as a function of the external temperature.

$$CoP_{H_2} = 1.6 \cdot \exp(-0.018 \cdot T_\infty) \tag{10}$$

It is important to remember that a number of variables, including the system's design, the surrounding temperature, and the hydrogen pressure, can have an impact on the energy performance of a hydrogen pre-cooling system. The overall layout of the hydrogen refueling station, including the size and arrangement of the storage tanks, as well as the type of dispenser employed, can also have an impact on the energy efficiency of a hydrogen pre-cooling system. It is also crucial to keep in mind that the quality of hydrogen can have an impact on the energy requirements and effectiveness of a hydrogen pre-cooling system. For example, high-pressure and low-temperature hydrogen will require less energy to cool than low-pressure and high-temperature hydrogen, since the enthalpy of the hydrogen flow changes according to pressure and temperature levels, as shown in Figure 11.

The ambient temperature and the chosen cooling technology will also have an impact on the energy usage and effectiveness of a hydrogen pre-cooling system. In a hydrogen fueling station, the hydrogen can be precooled using a variety of cooling technologies. The most typical types include:

1. Vapor-compression refrigeration is a popular form of cooling technology. It works by compressing a refrigerant, which absorbs heat from the hydrogen and releases it into the surrounding air. With the aid of this technology, hydrogen can be cooled to −40 °C.
2. Cryogenic cooling: This method chills hydrogen to extremely low temperatures, usually below −150 °C, using liquefied gases like liquid nitrogen or liquid helium. Larger hydrogen fueling stations based on liquid hydrogen storage could use cryogenic fluids.
3. Absorption cooling: This method cools hydrogen via the adoption of absorption chillers.

The best cooling technology for a particular application will depend on elements like the amount of hydrogen to be cooled, the desired cooling rate, and other considerations. Each of these technologies has its own benefits and drawbacks.
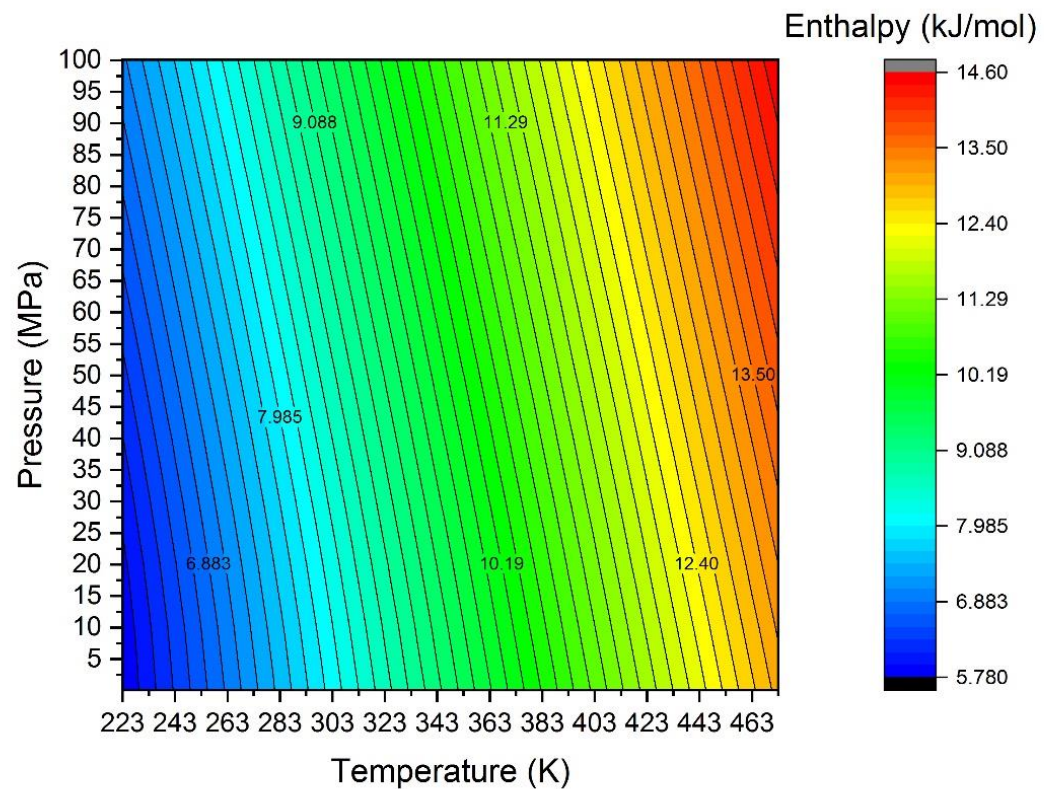
**Figure 11.** Enthalpy values for several pressure and temperature levels. Data processed from [40].

A Ranque–Hilsch vortex tube (RHVT) may be included in the precooling procedure used to fill high-pressure hydrogen cars at hydrogen refueling stations. Chen et al. [90] investigated the design of the precooling process for high-pressure hydrogen refueling by using two innovative precooling approaches with RHVT. The suggested solutions with RHVT integration to create cooling capacity have cheaper equipment investments and operating power costs than the typical hydrogen fueling process with a vapor-compression precooling unit.

Piraino et al. [91] analyzed the cooling performance at the Hydrogen Research and Fueling Facility, in Los Angeles. An individual −20 °C system with a coil chiller hanging in a chilled fluid drum served as the base cooling system for the initial facility design. This setup worked well for sporadic refuelings, but it struggled for several refuelings in hot and cold conditions. After the first cooling, a separate cooling system was built in series. The second cooling system comprises a condensing unit that can function at temperatures as low as 40 °C and a flat plate aluminum block evaporator heat exchanger. To reduce any heat absorptions in the lines, the heat exchanger is situated near the dispenser. Even in the warmest temperatures, this method eliminated any problems for many fuelings to ensure retail performance. Considering a different configuration, Xiao et al. [92] suggested a throttling valve and cooling-recovery venting mechanism for cryo-compressed hydrogen storage, which can extend the parking period.

When multiple refueling processes are performed consecutively, they are called "back-to-back" refueling processes [93]. In this scenario, the hydrogen pre-cooling system has to operate under severe conditions, since the low temperature has to be kept at the desired level for longer periods, as shown in Figure 12.
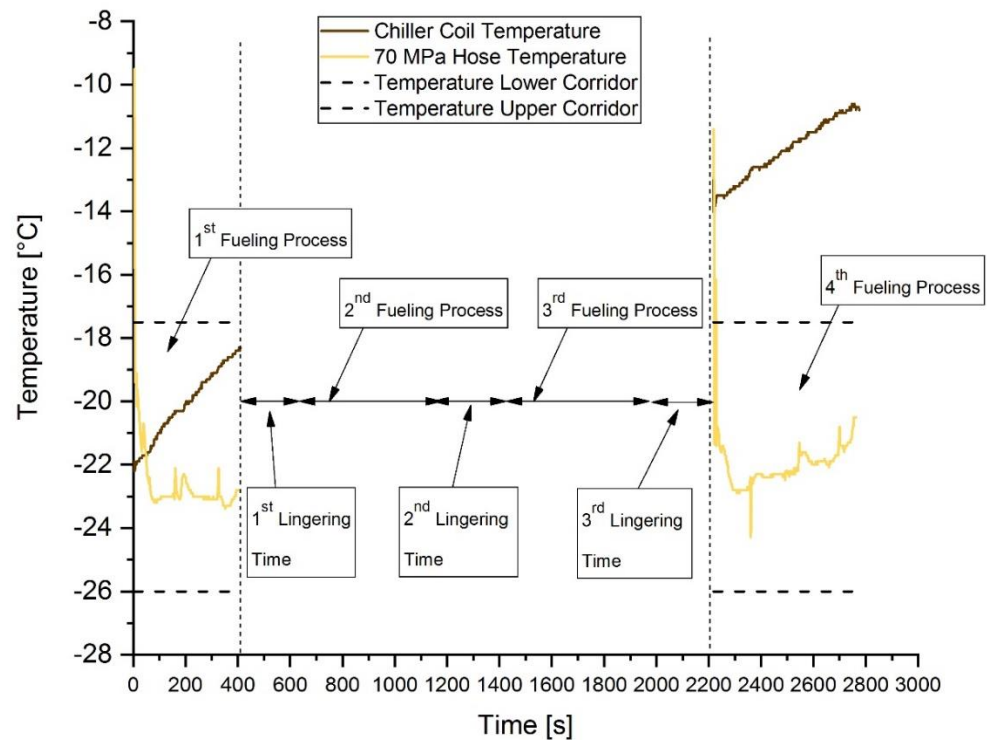
**Figure 12.** Four back-to-back refueling processes and temperature trend at the station. Reproduced with permission from [93], Elsevier, 2023.

*3.5. CCHS Filling*

The process of filling the CCHS is a complex procedure, studied at international level by several researchers and industrial realities. The energy balance of the CCHS fill can be described by Equation (11), neglecting the change in gravitational energy and considering that no work is produced/required during the filling process.

$$\dot{Q}_{exchanged} + \dot{m}_{in} \cdot \left( h_{in} + \frac{v_{in}^2}{2} \right) = \frac{d}{dt} \left[ m \cdot \left( u + \frac{v^2}{2} \right) \right] \tag{11}$$

The heat exchanged with the environment is affected by the geometry and the types of vehicle tanks, already described in Figure 5. Different materials present different heat transfer properties, as listed in Table 5.

**Table 5.** Heat transfer properties of different tank materials. Data retrieved from [94–99].

| Tank Material | Density (kg/m$^3$) | Specific Heat (J/(kg·K)) | Thermal Conductivity (W/(m·K)) |
|---|---|---|---|
| Aluminum liner | 2700–2730 | 902–900- | 167–238 |
| High-density polyethylene liner | 952 | 2090 | 0.3–0.42 |
| Carbon fiber/epoxy composite laminate | 1513–1494 | 920–938 | 3.72–1 |
| Glass fiber/epoxy composite laminate | 2051 | 878.4 | 0.133 |
| Steel | 8030 | 502.48 | 16.27 |

For a fuel cell electric vehicle, the state of charge (SOC) concept can be used to assess how well a refueling operation went. The ratio of the hydrogen density calculated at the final temperature and pressure to the density at 15 °C and 70 MPa is known as SOC.

$$SoC = \frac{\rho_{H_2}\left(T_{final}, p_{final}\right)}{\rho_{H_2}(15°C, 700 \text{ bar})} \tag{12}$$

The refueling procedure must take into account three main phenomena:

- The heat produced during compression, which may influence the hydrogen temperature level within the tank.
- The negative Joule–Thomson coefficient, which states that as the quantity of pressurized gas entering the tank rises, the temperature rises.
- The materials and wall thickness used to construct hydrogen storage tanks minimize heat transmission, which might affect the temperature increase in the tank.

For this reason, it is mandatory to avoid over-pressurization (usually the maximum pressure is identified as 125% of the nominal working pressure), overheating of the tank above 85 °C, and an overfill. Figure 13 shows the limits and the allowable areas for HRP at Nominal Working Pressures (NWP) of 350 bar (Figure 13a) and 700 bar (Figure 13b).
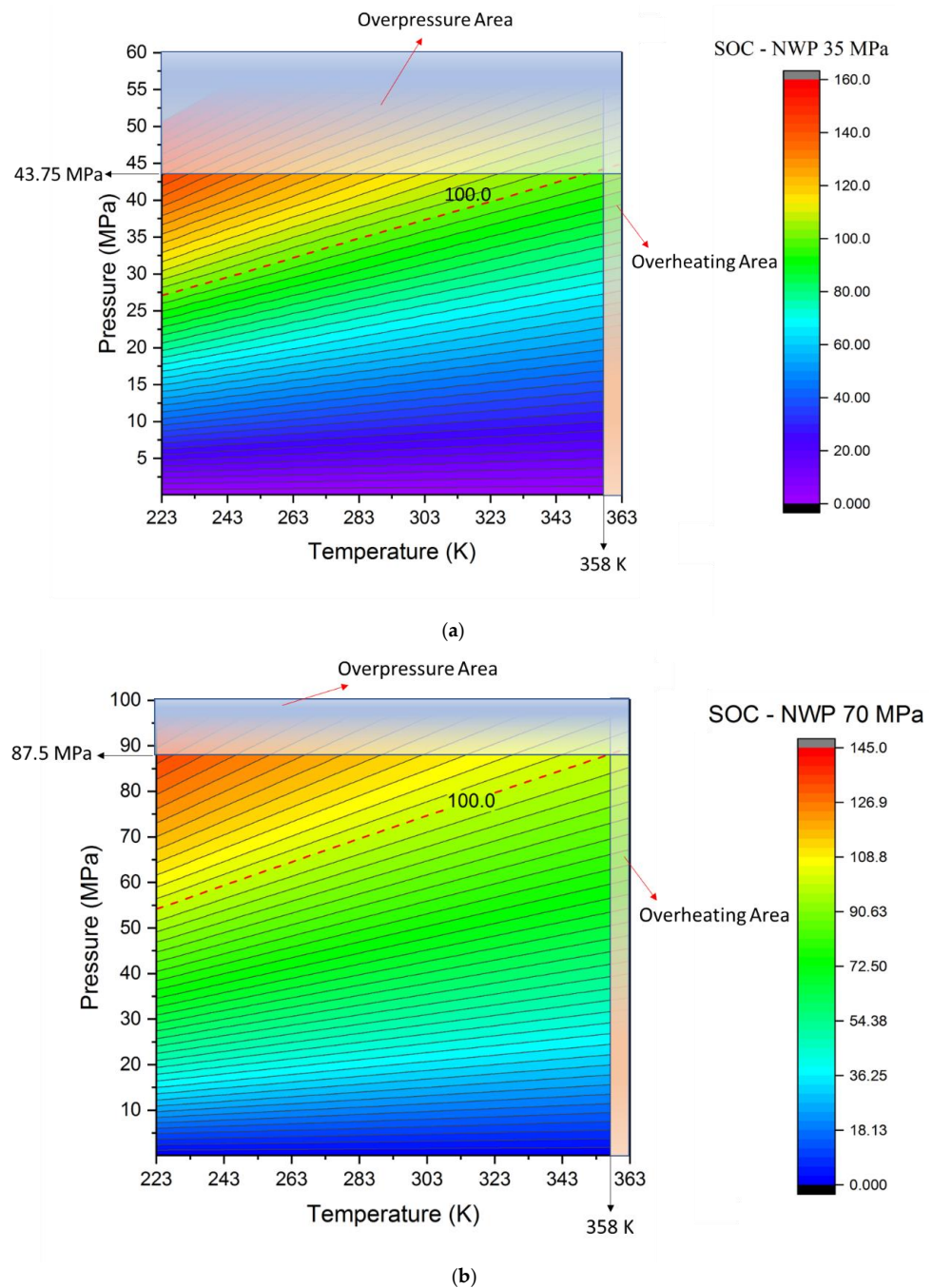


(a)



(b)

**Figure 13.** Allowable SOC values for 35 MPa (**a**) and 70 MPa (**b**).

Table 6 presents the main research activities so far carried out by the scientific community about CCHS filling procedures.

**Table 6.** Main research activities on CCHS filling.

| Authors | Year | Methods | Main Finding |
| --- | --- | --- | --- |
| Dicken and Mérida [100] | 2007 | Experimental analyses | Significant temperature variations were induced by the experimental settings with larger ratios of final to beginning mass. The highest rates of temperature increase, however, were produced by the lowest ratios. Due to buoyancy effects at lower gas input velocities, longer fill periods resulted in lower final average gas temperatures (relative to shorter fills) and a temperature field with substantial vertical stratification. |
| Kim et al. [101] | 2010 | CFD analyses | Analyses of the thermal flow characteristics of hydrogen filling and suggestions that further work needs to be done to ensure the safety of a type IV cylinder during filling procedures. |
| Zheng et al. [102] | 2010 | Multi-objective Optimization | In order to accomplish both rapid refueling and high utilization, a multi-objective iterative optimization model has been developed, and an optimization technique for the filling process has been provided. |
| Liu et al. [99] | 2010 | Experimental analyses | During the filling process, the temperature within the cylinder rises nonlinearly, with the caudal area seeing the highest temperature rise at the cylinder interface. |
| Zhao et al. [103] | 2010 | CFD analyses and experimental activities | As the filling rate and ambient temperature rise, the maximum temperature rises as well, whereas as the starting pressure rises, it decreases. |
| Li et al. [104] | 2012 | CFD analyses | Higher temperature increase is the effect of smaller inlet diameter, while refueling with a higher flow rate results in a smaller temperature increase. |
| Olmos and Manousiouthakis [105] | 2013 | Thermodynamic Model | Based on thermodynamics and transport principles, a new mathematical model captures hydrogen pressure, temperature, and molar volume changes during the refueling process. |
| Zheng et al. [106] | 2013 | CFD analyses and experimental activities | The findings indicate that the final hydrogen temperature reduces almost linearly when starting pressure is increased and the ambient temperature is lowered. |
| Rothuizen et al. [107] | 2013 | Thermodynamic Model | The total energy required for cooling may be decreased by 12% by employing numerous pressure stages in the tanks at the refueling station (instead of a single high-pressure tank), and the compressor power consumption can be decreased by 17%. The total volume of hydrogen held at high pressure is lowered by 20%, and the time between refueling is shortened by 5%. |
| Suryan et al. [108] | 2013 | CFD analyses | Comparative analysis of the effectiveness of turbulence models for refilling compressed hydrogen tanks. The most effective turbulence model for the issue of filling a hydrogen tank is the k-model. |
| Ruffio et al. [109] | 2014 | Multi-physic approach | Different ways are used and compared to deal with heat loss. First, a global thermal conductance is defined, which lets analytical expressions be made. Then, to take into account the effects of thermal capacity, a thermal nodal modeling of the tank walls is suggested. A 1D model of the tank walls that is almost infinite is shown. Lastly, this model is used to find the best mass flow rate so that the filling process doesn't cause the temperature to rise too much. |
| Wang et al. [110] | 2014 | CFD Analyses | The results of the simulation show that there is a linear or inverse proportional relationship between the mass of the filling and the initial temperature and pressure, and the filling rate. By looking at how adiabatic and diathermal filling affects the state of charge, a formula to study heat transfer is proposed. |
| Cebolla et al. [111] | 2015 | Experimental analysis | To explore the impact of liner materials, two tanks (types 3 and 4) were employed. By lowering the temperature of the incoming gas, the energy content of the tank increased while using less energy overall. |

**Table 6.** *Cont.*

| Authors | Year | Methods | Main Finding |
|---|---|---|---|
| Bourgeois et al. [112] | 2015 | Thermodynamic model and experimental activities | A new relationship between the gas and wall's heat exchange as a function of Reynolds Number. |
| de Miguel et al. [113] | 2016 | CFD analysis | CFD simulations are carried out to better understand the influence of the key processes on the gas temperature histories, such as gas compression, gas mixing, and heat transfer. |
| de Miguel et al. [114] | 2016 | Experimental analyses | The findings suggested that greater gas temperature disparities are brought on by larger opening sizes and slower filling. The so-called "gas temperature stratification", a vertical temperature gradient, is what causes the temperature inhomogeneity, with the maximum temperature value found close to the tank's top. One of the two primary processes influencing gas behavior in the tank—gas turbulence or buoyancy—can be used to explain the ultimate distribution of gas temperatures. |
| Xiao et al. [115] | 2016 | Thermodynamic Model | Analytic estimates for the temperature and pressure levels using a basic thermodynamic technique. |
| Xiao et al. [116] | 2016 | Thermodynamic Model | The parameters of refueling, such as final hydrogen temperature, ambient temperature, initial temperature, and additional parameters, can be used to determine the temperature of the hydrogen before cooling. |
| Cheng et al. [117] | 2017 | Thermodynamic Model | Lumped parameter models, obtaining fitting curves for final hydrogen temperature levels. |
| Wang et al. [118] | 2017 | Thermodynamic Model | Lumped parameter models, obtaining fitting curves for final hydrogen mass levels. |
| Xiao et al. [119] | 2017 | Fitting curves | Based on the law of mixtures, the analytical solution's ending hydrogen temperature is a weighted average of starting, intake, and ambient temperatures. |
| Bourgeois et al. [120] | 2017 | CFD analyses and experimental activities | Validating models required 82 instrumented Type 4 and Type 3 vessel filling and emptying experiments. The gas-to-wall heat transfer coefficient was calculated from temperature readings using new methodologies. CFD models analyzed temperature differences and replicated thermal stratification under particular filling situations. |
| Kuroki et al. [121] | 2018 | Thermodynamic Model | The suggested method simulates a hydrogen refueling process and predicts the transient hydrogen temperature, pressure, and mass flow rate. |
| Kuroki et al. [122] | 2018 | Thermodynamic Model | To foresee an increase in hydrogen temperature while being refueled, the authors suggested a thermodynamic analytical technique, by considering the filling apparatus to be a straightforward pipeline. |
| Xiao et al. [123] | 2018 | Thermodynamic Model | For both a 35 MPa and a 70 MPa tank with various volumes, the impacts of three single parameters—the ambient temperature, the beginning pressure, and the mass flow rate—on the ending hydrogen temperature are investigated. |
| Xiao et al. [124] | 2019 | Thermodynamic Model | Using two distinct temperatures for the gas zone and the wall zone, the authors expanded the single-zone model to create the dual-zone model. |
| Melido et al. [125] | 2019 | CFD analysis | The likelihood of generating gas temperature in-homogeneities increases with the initial temperature (longer filling time, slower filling velocity). The gas temperature differential between the top and lower regions grows linearly with the starting temperature when stratification takes place. |
| Li et al. [96] | 2019 | Review | Review and analysis of the theoretical research, tests, and simulations on the rapid refueling-related parameters, including starting pressure, initial temperature, refilling rate, and ambient temperature |
| Sapre et al. [126] | 2019 | CFD analysis | This study presents the results of an adiabatic simulation of the Type IV tank refueling procedure at a nominal operating pressure of 70 MPa. The findings showed that refueling factors, particularly supply hydrogen temperature and filling rate, had a substantial impact on end temperature and state of charge. |

**Table 6.** *Cont*.

| Authors | Year | Methods | Main Finding |
|---|---|---|---|
| Zhou et al. [127] | 2019 | Thermodynamic Model | Lumped parameter models, obtaining fitting curves for a refueling time as a function of filling parameters. |
| Wang et al. [128] | 2019 | Thermodynamic Model | The research focused on the impacts of mass flow rate and heat transfer coefficient on hydrogen filling performance. |
| Liu et al. [129] | 2020 | CFD analysis | Simulation of 150 L on-bus gaseous hydrogen storage cylinder, including the NWP of 35 and 70 MPa and the filling duration of 3 and 5 min. The findings demonstrate that for various types of cylinders, "the region of the head dome junction or the caudal portion of the cylinder" may be where the largest temperature increase occurs. |
| Jiang et al. [130] | 2020 | CFD and FEM analysis | During the filling process, a method for analyzing the fluid-thermal-solid coupling is proposed. First, a CFD model of the temperature field is set up. The second step is to build a finite element model to study the thermal-mechanical behavior. During fast filling, the rate of filling can change the temperature and the stress field. The temperature field will be different depending on where the air comes in. |
| Wang and Decès-Petit [131] | 2020 | Machine Learning | Using machine learning techniques to forecast the level of charge, which is the primary performance goal of the fueling process. Three hydrogen refueling stations with up to two years of operating data were used in the tests. In three locations, the categorization accuracy exceeded 85%. |
| Deng et al. [132] | 2020 | Thermodynamic Model | A single-zone lumped parameter model of the vehicle's hydrogen tank provides the analytical approximation for the final hydrogen temperature. With respect to the beginning temperature, inflow temperature, and ambient temperature, the authors provide the expression of the final hydrogen temperature. |
| Wen et al. [133] | 2020 | CFD analyses | The energy efficiency is increased by using less hydrogen from the high-pressurized hydrogen storage during vehicle refueling when an ejector rather than a reduction valve is included in the hydrogen fueling station. |
| Rothuizen et al. [134] | 2020 | Thermodynam-ic Model in Dimola | The ending temperature in the CHSS stays consistent regardless of the APRR assuming there are no pressure losses in the vehicle. As the pressure loss is directly correlated to the mass flow rate, which is lessened by lower APRRs, if there are pressure losses in the CHSS, the lower the APRR, the smaller the temperature rise. The research highlights how crucial it is to keep pressure loss inside the vehicle to a minimum in order to increase APRR and get quicker fueling times without jeopardizing boundary conditions. |
| Sapre et al. [135] | 2021 | Regression Model | The effect of refueling variables on the Type IV tank's storage density has been researched. The storage density of the tank is significantly influenced by the filling rate, filling time, end temperature/pressure, and hydrogen supply temperature, which were all recognized as substantial contributors. |
| Caponi et al. [136] | 2021 | Thermodynamic Model | Considering fuel cell electric buses, at the end of the refueling, the gas temperature reached 313.3 K and the target pressure has been reached after 633 s. The gas heating in the tank follows a non-linear shape. |
| Kuroki et al. [137] | 2021 | Thermodynamic Model | The model determines the variations in hydrogen temperature, pressure, and mass flow rate at every point in the fueling process by first solving the energy and mass balances at each component in the system. The accuracy of the model is evaluated against experimental data gathered at National Renewable Energy Lab. |
| Li et al. [138] | 2021 | Lumped parameters and FEM analyses | The findings demonstrated that the infill may over-suppress gas convection. Thermal stratification may cause local overheating in gas tanks with considerable temperature differences. This analysis discovered the hot region above the gas tank intake. |
| Genovese et al. [93] | 2021 | Experimental analyses | Analyses of back-to-back refueling process, evaluation of temperature profile, vehicle state of charge, and dynamic cooling operation. |

**Table 6.** *Cont.*

| Authors | Year | Methods | Main Finding |
|---|---|---|---|
| Bai et al. [139] | 2021 | Multi-objective Optimization | Pressure switching coefficient affects filling time, while hydrogen pre-cooling affects cylinder temperature increase and SOC. In cascade hydrogen refueling, a multi-objective iterative optimization approach is developed to determine the pressure switching coefficient and hydrogen pre-cooling temperature to speed up refueling, minimize energy consumption, and increase cylinder SOC. |
| Wu et al. [140] | 2021 | CFD analyses | To satisfy the need to reduce the filling time as much as feasible without going over the maximum temperature limit, several time-delayed filling solutions are provided for different situations based on the regulation of mass flow rate. In a typical context, the suggested technique may finish the filling in 155 s, which is 62% faster than filling at a constant mass flow rate. |
| Oh. et al. [95] | 2022 | CFD analysis | To validate the numerical approach and establish the connection between Nu and Re numbers, experimental data and numerical analysis data were compared. As a consequence, Nusselt and Reynolds' relationship |
| Wang et al. [141] | 2022 | Machine Learning | Black-box machine learning model to discover the correlation between the initial operating parameters and the end fueling process parameters. At each point throughout the fueling process, the ultimate temperature, pressure, and SOC can be predicted using this model. |
| Kawatsu et al. [142] | 2022 | Dynamic physical model in Modelica | The model, which reflects the station's design and operational conditions, was used to show a quantitative assessment of the dynamic behavior of hydrogen during refueling operations. Comparatively to the traditional risk analysis approach, this characteristic of the suggested model also offers a physical and realistic dynamic leakage rate for estimating individual risks. |
| Chen et al. [143] | 2022 | Thermodynamic Model | Results obtained show that using a turbo-expander might save precooling energy use by 52.6%. Additionally, the infrastructure cost of the suggested procedure is around 210,000 dollars less than the traditional one. |
| Park and Chae [144] | 2022 | Machine Learning | By using various coefficients, a polynomial equation is provided with regard to temperature and pressure in order to exhibit distinct hydrogen thermo-physical characteristics. A machine learning technique is used to regress the equation and calculate the coefficients using a large amount of reference data. |
| Li et al. [145] | 2022 | Experimental and CFD analyses | The temperature increase within the hydrogen tank may be efficiently suppressed by tuning pre-cooling and filling rate methods. |
| Luo et al. [54] | 2022 | Artificial neural network | According to the study, adopting the ideal starting pressure and capacity of the cascade storage tanks may minimize the cooling energy consumption by up to 11.43% when the ambient temperature is 293.15 K and the SOC is 0.98–0.99. |
| Deng et al. [146] | 2023 | Thermodynamic Model | A dual-zone lumped parameter model that separates the tank into hydrogen gas and tank wall zones is proposed using Matlab/Simulink. The lumped parameter model simulates the SAE J2601 MC Default method hydrogen filling beginning circumstances. |

## 4. Refuelling Procedures

To ensure the safety of the vehicle and the station, hydrogen vehicles must adhere to all applicable safety regulations and standards. Tanks and entire systems must be designed, produced, and tested to meet these requirements. Recently, Genovese et al. [147] presented an overview of the current standards and protocols for the operation of an HRS, including the refueling protocols.

In general, there are three main possibilities for the refueling procedures:

1. Imposing the ramp rate, via the adoption of an APRR. In this case, the pressure profile is monitored and controlled, as described in Equation (13). The mass flow rate dispensed to the vehicle is a non-controlled variable, only monitored. The temperature profile could be either actively monitored and controlled, or only used as a parameter to end the refueling procedure.

$$\frac{dp}{dt} = f(APRR) \tag{13}$$

2. Imposing the mass flow rate and monitoring the temperature profile for fast filling. In this configuration, the pressure ramp rate is a non-controlled variable, only monitored. The temperature profile could be either actively monitored and controlled, or only used as a parameter to end the refueling procedure.

$$\frac{dm}{dt} = f\left(\dot{m}_{fueling}\right) \tag{14}$$

3. A combination of the previous procedures, to be adopted under certain circumstances and for a portion of the refueling process. E.g., imposing the mass flow rate for faster fueling at the beginning and then imposing the pressure ramp rate for avoiding excessive overheating.

Currently, most of the refueling standards adopt the adoption of the look-up table approach to identify and impose the proper APRR values. An example of such an application is the SAE J2601, for light-duty vehicles [148]. Figure 14 shows an example of a refueling process with an imposed APRR of 15 MPa/min for a light-duty vehicle, with two different pre-cooling temperatures, namely of 0 °C and −40 °C, achieving a target SOC of 97%. Notably, a pre-cooling of 0 °C does not prevent overheating above the temperature limit of 85 °C when simulating a ramp rate similar to the one simulated.

The refueling process has been extensively investigated in the literature. Maus et al. [149], in 2008, first presented the theory and the concept of hydrogen refueling procedures. Recently, several authors proposed new approaches to meet the new HRS layouts and needs, such as HRSs with liquid storage, or less energy demanding equipment.

Wang et al. [150] analyzed refueling processes and their technical performance. The authors highlighted appropriate mitigation measures and solutions to limit or mitigate the effects of temperature rise are proposed, such as pre-cooling the hydrogen in advance, lowering the initial hydrogen content in the tank, and making sure that the ambient temperature and initial tank temperature are at a low level. Due to the inefficiency of various hydrogen refueling protocols in terms of application scope and application techniques, several new protocols have the potential to innovate in this field. The construction of a hydrogen refueling station is quite expensive and involves taking into account a number of factors, including location, economics, dangers, etc. Establishing a thorough planning strategy for new hydrogen filling stations is important.

Ku et al. [151] modified the "Heavy Duty Refueling Station Analysis Model" (HDR-SAM) tool to analyze the submerged cryopump installation in an HRS, for heavy-duty vehicle refueling. By evaluating two hydrogen storage systems, compressed gas, and metal hydride storage, Apostolou [152] examined the economical elements of the refueling operations of a light-duty urban vehicle, such as a fuel cell bus. The key findings demonstrated that metal hydride configuration might provide customers with less expensive fuel, but with longer refueling intervals, and could generate a lucrative investment for future investors. Li et al. [153] showed a hydrogen refueling system is capable of supplying precooled, compressed gaseous hydrogen for heavy-duty vehicle refueling applications. The system complies with SAE J2601 standards by using a submerged pump to transfer pressurized liquid hydrogen from a cryogenic storage tank to a dispensing control loop. The control loop then vaporizes the liquid and modifies the pressure and temperature of the

resulting gas to enable refueling at 35 MPa and as low as −40 °C. The European PRHYDE ("PRotocol for heavy-duty HYDrogEn refueling") study concentrates on the innovations needed for refueling medium- and heavy-duty hydrogen vehicles [154].
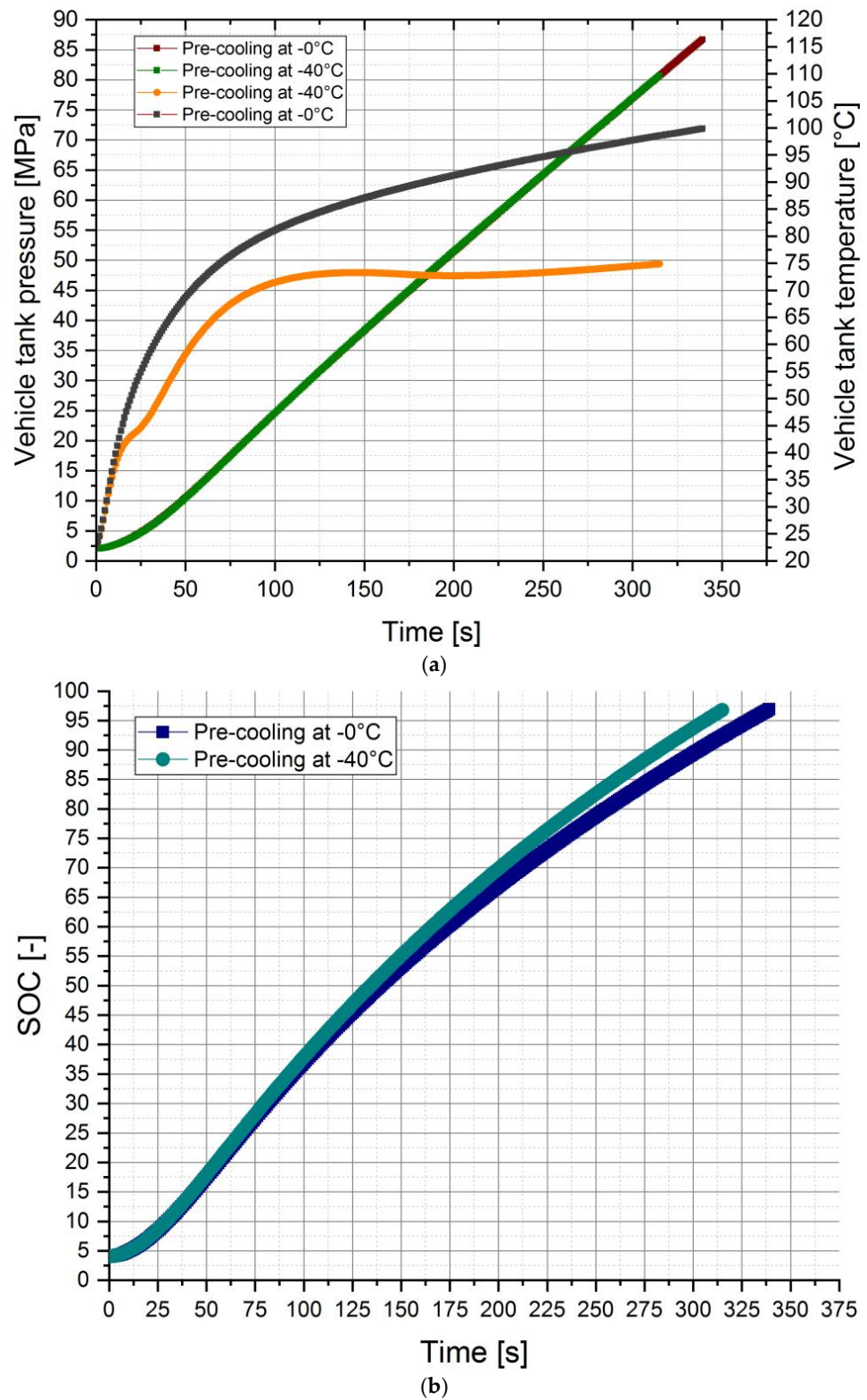


**Figure 14.** Pressure and temperature profiles (**a**), and SOC profile (**b**), for a refueling process with imposed APRR, calculated via the adoption of the H2Fills Tool [137].

LaChance et al. [155], in 2009, provided a method for risk-informing the permitting procedure for hydrogen fueling stations. The mentioned method principally depends on the creation of risk-informed codes and standards. Böhm et al. [156] analyzed concepts and refueling procedures for railway applications. During refilling, heat from the refueling station, the vehicle's thermal masses, the Joule–Thomson heating of hydrogen during throttling via the fuel line orifices, and compression heat raise the hydrogen temperature in the tank storage system. After 15 min fills and pre-cooling at $-20\ ^\circ$C, SoC approaches 100%. At ambient temperatures of 40 $^\circ$C, 350 L 35 MPa storage cylinders overheat in simulations. 50 L tank layouts have a larger heat exchange exterior surface area than 350 L tank configurations, resulting in 10 $^\circ$C lower temperatures. Type III tanks have a lower ultimate filling temperature than type IV tanks because aluminum has a greater heat transfer coefficient.

Petitpas et al. [157,158] analyzed a new concept of hydrogen refueling procedure. Instead of depending on compressors, this method stores liquid hydrogen in cryogenic pressure tanks where pressurization happens by heat transfer. Thermal compression appeals to early market applications because of its capacity flexibility (broad range of pressure, temperature, and station demand).

Charolais et al. [159] suggested a new "Safety Watchdog" approach as a way to make sure that different protocols, both those already in use and those that could be used in the future, are safe. This "Safety Watchdog" checks the limits of the fueling process without being controlled by the main process controls. By separating the watchdog from the protocol, it is possible to use more cost-effective protocols while still making sure that all safety conditions are met.

Xu et al. [56] optimized the gaseous HRS process and control mechanism for rapid, efficient refueling to minimize energy consumption and enhance daily fueling capacity. Experimental results showed just a 2 $^\circ$C temperature increase error for a typical refueling event using a dynamic HRS model utilizing numerical methods. Optimized heavy-duty FCV refueling procedures showed an average fueling rate of 2 kg/min and pre-cooling consumption of less than 7 kW for 35 MPa type III tanks.

Striednig et al. [160] developed a thermodynamic model, and with the use of experimental data, the simulation findings for type I tanks were verified, and a refueling procedure for hydrogen-powered industrial vehicles was proposed, with ramp rates up to 34.5 MPa/min. Moreno-Blanco et al. [161] considered delivering cold (200 K) high-pressure (875 bar) hydrogen in insulated trailers and discharging it directly from the trailer, which could completely remove the station equipment, reducing station complexity and enhancing functionality by allowing virtually unlimited back-to-back fueling processes. Petitpas et al. [162] offered the first thorough assessment of cryogenic pressurized vessel fill density as a function of starting thermodynamic state and liquid hydrogen pump performance, which is essential for evaluating this promising technology. In conclusion, pumping liquid hydrogen is a potential approach for dispensing in cryogenic and moderate temperature vessels, guaranteeing high throughput (1.67 kg/min, 100 kg/h), infinite capacity for back-to-back refueling, low station energy usage owing to high density decreasing compression effort.

## 5. Conclusions

The purpose of this study is to provide a comprehensive understanding of the current status of HRPs, as well as their general methods and the technical obstacles they face.

The literature review that was conducted for the purpose of this work assisted in identifying the research topics of interest, which include storage, dispensing lines, pressure regulators, pre-cooling, vehicle filling processes, and refueling procedures. As a consequence of this, the paper is broken up into six sections, in which the most recent research activities for each topic area will be discussed, with an emphasis placed not only on the theory that guides the study but also on the innovations provided by the numerous research groups that have been investigated.

The following conclusions can be drawn:

- Concerning hydrogen storage, the majority of the research efforts are concentrated on establishing the optimal design for cascade hydrogen storage systems with the goal of reducing the amount of energy that is wasted by either the HRP or the irreversibilities.
- In the hydrogen dispensing line, pulsation-free operation, pressure losses, and hydrogen losses are the most critical aspects that must be addressed.
- The Joule–Thomson phenomenon has a predominant effect affecting the temperature level after the pressure regulator.
- Pre-cooling systems are necessary equipment to perform a fast refueling process without overheating the gas. This is especially true for back-to-back refueling processes.
- Modeling and testing CCHS filling have been performed via different methodologies by researchers. The most key findings have been summarized.
- Current refueling procedures consider the imposition of an APRR to perform the filling process.

The results provided in this research have the potential to serve as a rock-solid foundation for future enhancements and studies, helping researchers to define and excel in the examination and analysis of high-performance HRPs and related HRSs.

## References

1. Hassan, I.A.; Ramadan, H.S.; Saleh, M.A.; Hissel, D. Hydrogen Storage Technologies for Stationary and Mobile Applications: Review, Analysis and Perspectives. *Renew. Sustain. Energy Rev.* **2021**, *149*, 111311. [CrossRef]
2. Kovač, A.; Paranos, M.; Marciuš, D. Hydrogen in Energy Transition: A Review. *Int. J. Hydrogen Energy* **2021**, *46*, 10016–10035. [CrossRef]
3. Cigolotti, V.; Genovese, M.; Fragiacomo, P. Comprehensive Review on Fuel Cell Technology for Stationary Applications as Sustainable and Efficient Poly-Generation Energy Systems. *Energies* **2021**, *14*, 4963. [CrossRef]
4. Genovese, M.; Schlüter, A.; Scionti, E.; Piraino, F.; Corigliano, O.; Fragiacomo, P. Power-to-Hydrogen and Hydrogen-to-X Energy Systems for the Industry of the Future in Europe. *Int. J. Hydrogen Energy* **2023**. [CrossRef]
5. Fragiacomo, P.; Genovese, M.; Piraino, F.; Corigliano, O.; de Lorenzo, G. Hydrogen-Fuel Cell Hybrid Powertrain: Conceptual Layouts and Current Applications. *Machines* **2022**, *10*, 1121. [CrossRef]
6. Fragiacomo, P.; Piraino, F.; Genovese, M.; Corigliano, O.; Lorenzo, G. de Strategic Overview on Fuel Cell-Based Systems for Mobility and Electrolytic Cells for Hydrogen Production. *Procedia Comput. Sci.* **2022**, *200*, 1254–1263. [CrossRef]
7. Elgowainy, A.; Gaines, L.; Wang, M. Fuel-Cycle Analysis of Early Market Applications of Fuel Cells: Forklift Propulsion Systems and Distributed Power Generation. *Int. J. Hydrogen Energy* **2009**, *34*, 3557–3570. [CrossRef]
8. Lototskyy, M.V.; Tolj, I.; Parsons, A.; Smith, F.; Sita, C.; Linkov, V. Performance of Electric Forklift with Low-Temperature Polymer Exchange Membrane Fuel Cell Power Module and Metal Hydride Hydrogen Storage Extension Tank. *J. Power Sources* **2016**, *316*, 239–250. [CrossRef]
9. Jones, J.; Genovese, A.; Tob-Ogu, A. Hydrogen Vehicles in Urban Logistics: A Total Cost of Ownership Analysis and Some Policy Implications. *Renew. Sustain. Energy Rev.* **2020**, *119*, 109595. [CrossRef]
10. Sagaria, S.; Costa Neto, R.; Baptista, P. Assessing the Performance of Vehicles Powered by Battery, Fuel Cell and Ultra-Capacitor: Application to Light-Duty Vehicles and Buses. *Energy Convers. Manag.* **2021**, *229*, 113767. [CrossRef]
11. Breuer, J.L.; Samsun, R.C.; Stolten, D.; Peters, R. How to Reduce the Greenhouse Gas Emissions and Air Pollution Caused by Light and Heavy Duty Vehicles with Battery-Electric, Fuel Cell-Electric and Catenary Trucks. *Environ. Int.* **2021**, *152*, 106474. [CrossRef] [PubMed]
12. Di Ilio, G.; di Giorgio, P.; Tribioli, L.; Cigolotti, V.; Bella, G.; Jannelli, E. Assessment of a Hydrogen-Fueled Heavy-Duty Yard Truck for Roll-On and Roll-Off Port Operations. In *SAE Technical Papers*; SAE International: Warrendale PA, USA, 5 September 2021.

13. Di Ilio, G.; di Giorgio, P.; Tribioli, L.; Bella, G.; Jannelli, E. Preliminary Design of a Fuel Cell/Battery Hybrid Powertrain for a Heavy-Duty Yard Truck for Port Logistics. *Energy Convers. Manag.* **2021**, *243*, 114423. [CrossRef]

14. De las Nieves Camacho, M.; Jurburg, D.; Tanco, M. Hydrogen Fuel Cell Heavy-Duty Trucks: Review of Main Research Topics. *Int. J. Hydrogen Energy* **2022**, *47*, 29505–29525. [CrossRef]

15. Piraino, F.; Fragiacomo, P. A Multi-Method Control Strategy for Numerically Testing a Fuel Cell-Battery-Supercapacitor Tramway. *Energy Convers. Manag.* **2020**, *225*, 113481. [CrossRef]

16. Fragiacomo, P.; Piraino, F. Fuel Cell Hybrid Powertrains for Use in Southern Italian Railways. *Int. J. Hydrogen Energy* **2019**, *44*, 27930–27946. [CrossRef]

17. Samsun, R.C.; Rex, M.; Antoni, L.; Stolten, D. Deployment of Fuel Cell Vehicles and Hydrogen Refueling Station Infrastructure: A Global Overview and Perspectives. *Energies* **2022**, *15*, 4975. [CrossRef]

18. Can Samsun, R.; Antoni, L.; Rex, M.; Stolten, D. *Deployment Status of Fuel Cells in Road Transport: 2021 Update*; Forschungszentrum Jülich GmbH Zentralbibliothek: Jülich, Germany, 2021.

19. Genovese, M.; Fragiacomo, P. Hydrogen Refueling Station: Overview of the Technological Status and Research Enhancement. *J. Energy Storage* **2023**, *61*, 106758. [CrossRef]

20. Hydrogen Europe Hydrogen Europe, Committee Votes on AFIR, Maritime Transport. Available online: https://hydrogeneurope. eu/committee-votes-on-afir-maritime-transport/ (accessed on 20 January 2023).

21. Kang, J.E.; Brown, T.; Recker, W.W.; Samuelsen, G.S. Refueling Hydrogen Fuel Cell Vehicles with 68 Proposed Refueling Stations in California: Measuring Deviations from Daily Travel Patterns. *Int. J. Hydrogen Energy* **2014**, *39*, 3444–3449. [CrossRef]

22. Muratori, M.; Bush, B.; Hunter, C.; Melaina, M.W. Modeling Hydrogen Refueling Infrastructure to Support Passenger Vehicles. *Energies* **2018**, *11*, 1171. [CrossRef]

23. Pagliaro, M.; Iulianelli, A. Hydrogen Refueling Stations: Safety and Sustainability. *Gen. Chem.* **2020**, *6*, 190029. [CrossRef]

24. Kurtz, J.; Sprik, S.; Bradley, T.H. Review of Transportation Hydrogen Infrastructure Performance and Reliability. *Int. J. Hydrogen Energy* **2019**, *44*, 12010–12023. [CrossRef]

25. Kurtz, J.; Sprik, S.; Peters, M.; Bradley, T.H. Retail Hydrogen Station Reliability Status and Advances. *Reliab. Eng. Syst. Saf.* **2020**, 106823. [CrossRef]

26. Schneider, J. *SAE J2601-Worldwide Hydrogen Fueling Protocol: Status, Standardization & Implementation—SAE Fuel Cell Interface Group Chair*, PPT presentation, California Energy Commission, 13 August 2012. 2012.

27. Reddi, K.; Elgowainy, A.; Rustagi, N.; Gupta, E. Impact of Hydrogen Refueling Configurations and Market Parameters on the Refueling Cost of Hydrogen. *Int. J. Hydrogen Energy* **2017**, *42*, 21855–21865. [CrossRef]

28. Reddi, K.; Elgowainy, A.; Rustagi, N.; Gupta, E. Impact of Hydrogen SAE J2601 Fueling Methods on Fueling Time of Light-Duty Fuel Cell Electric Vehicles. *Int. J. Hydrogen Energy* **2017**, *42*, 16675–16685. [CrossRef]

29. Research and Market. *Global Market for Hydrogen Fueling Stations, 2019*; Report "Research and Market": Dublin, Ireland, 2019.

30. Wen, C.; He, G. Hydrogen Station Technology Development Review through Patent Analysis. *Clean Energy* **2018**, *2*, 29–36. [CrossRef]

31. Mayyas, A.; Mann, M. Manufacturing Competitiveness Analysis for Hydrogen Refueling Stations. *Int. J. Hydrogen Energy* **2019**, *44*, 9121–9142. [CrossRef]

32. Van Eck, N.J.; Waltman, L. Visualizing Bibliometric Networks. In *Measuring Scholarly Impact: Methods and Practice*; Ding, Y., Rousseau, R., Wolfram, D., Eds.; Springer International Publishing: Cham, Switzerland, 2014; pp. 285–320. ISBN 978-3-319-10377-8.

33. VOSviewer. Centre for Science and Technology Studies, Leiden University, The Netherlands. Available online: https://www. vosviewer.com (accessed on 25 January 2023).

34. Alazemi, J.; Andrews, J. Automotive Hydrogen Fuelling Stations: An International Review. *Renew. Sustain. Energy Rev.* **2015**, *48*, 483–499. [CrossRef]

35. Apostolou, D.; Xydis, G. A Literature Review on Hydrogen Refuelling Stations and Infrastructure. Current Status and Future Prospects. *Renew. Sustain. Energy Rev.* **2019**, *113*, 109292. [CrossRef]

36. Reddi, K.; Elgowainy, A.; Rustagi, N.; Gupta, E. Techno-Economic Analysis of Conventional and Advanced High-Pressure Tube Trailer Configurations for Compressed Hydrogen Gas Transportation and Refueling. *Int. J. Hydrogen Energy* **2018**, *43*, 4428–4438. [CrossRef]

37. Reddi, K.; Mintz, M.; Elgowainy, A.; Sutherland, E. Challenges and Opportunities of Hydrogen Delivery via Pipeline, Tube-Trailer, LIQUID Tanker and Methanation-Natural Gas Grid. In *Hydrogen Science and Engineering: Materials, Processes, Systems and Technology*; Wiley Online Library: Hoboken, NJ, USA, 2016; ISBN 9783527674268.

38. Abdalla, A.M.; Hossain, S.; Nisfindy, O.B.; Azad, A.T.; Dawood, M.; Azad, A.K. Hydrogen Production, Storage, Transportation and Key Challenges with Applications: A Review. *Energy Convers. Manag.* **2018**, *165*, 602–627. [CrossRef]

39. Faye, O.; Szpunar, J.; Eduok, U. A Critical Review on the Current Technologies for the Generation, Storage, and Transportation of Hydrogen. *Int. J. Hydrogen Energy* **2022**, *47*, 13771–13802. [CrossRef]

40. NIST Chemistry WebBook Thermophysical Properties of Hydrogen. Available online: https://webbook.nist.gov/cgi/fluid.cgi? ID=C1333740&Action=Page (accessed on 15 January 2023).

41. Farzaneh-Gord, M.; Deymi-Dashtebayaz, M.; Rahbari, H.R.; Niazmand, H. Effects of Storage Types and Conditions on Compressed Hydrogen Fuelling Stations Performance. *Int. J. Hydrogen Energy* **2012**, *37*, 3500–3509. [CrossRef]

42. Rothuizen, E.; Rokni, M. Optimization of the Overall Energy Consumption in Cascade Fueling Stations for Hydrogen Vehicles. *Int. J. Hydrogen Energy* **2014**, *39*, 582–592. [CrossRef]

43. Elgowainy, A.; Reddi, K.; Sutherland, E.; Joseck, F. Tube-Trailer Consolidation Strategy for Reducing Hydrogen Refueling Station Costs. *Int. J. Hydrogen Energy* **2014**, *39*, 20197–20206. [CrossRef]

44. Reddi, K.; Elgowainy, A.; Sutherland, E. Hydrogen Refueling Station Compression and Storage Optimization with Tube-Trailer Deliveries. *Int. J. Hydrogen Energy* **2014**, *39*, 19169–19181. [CrossRef]

45. Sakoda, N.; Onoue, K.; Kuroki, T.; Shinzato, K.; Kohno, M.; Monde, M.; Takata, Y. Transient Temperature and Pressure Behavior of High-Pressure 100 MPa Hydrogen during Discharge through Orifices. *Int. J. Hydrogen Energy* **2016**, *41*, 17169–17174. [CrossRef]

46. Talpacci, E.; Reuβ, M.; Grube, T.; Cilibrizzi, P.; Gunnella, R.; Robinius, M.; Stolten, D. Effect of Cascade Storage System Topology on the Cooling Energy Consumption in Fueling Stations for Hydrogen Vehicles. *Int. J. Hydrogen Energy* **2018**, *43*, 6256–6265. [CrossRef]

47. Reddi, K.; Elgowainy, A.; Rustagi, N.; Gupta, E. Two-Tier Pressure Consolidation Operation Method for Hydrogen Refueling Station Cost Reduction. *Int. J. Hydrogen Energy* **2018**, *43*, 2919–2929. [CrossRef]

48. Sadi, M.; Deymi-Dashtebayaz, M. Hydrogen Refueling Process from the Buffer and the Cascade Storage Banks to HV Cylinder. *Int. J. Hydrogen Energy* **2019**, *44*, 18496–18504. [CrossRef]

49. Kawano, Y.; Kuroki, T.; Sakoda, N.; Monde, M.; Takata, Y. Thermal Analysis of High-Pressure Hydrogen during the Discharging Process. *Int. J. Hydrogen Energy* **2019**, *44*, 27039–27045. [CrossRef]

50. Rogié, B.; Wen, C.; Kærn, M.R.; Rothuizen, E. Optimisation of the Fuelling of Hydrogen Vehicles Using Cascade Systems and Ejectors. *Int. J. Hydrogen Energy* **2021**, *46*, 9567–9579. [CrossRef]

51. Xiao, L.; Chen, J.; Wu, Y.; Zhang, W.; Ye, J.; Shao, S.; Xie, J. Effects of Pressure Levels in Three-Cascade Storage System on the Overall Energy Consumption in the Hydrogen Refueling Station. *Int. J. Hydrogen Energy* **2021**, *46*, 31334–31345. [CrossRef]

52. Xiao, J.; Bi, C.; Bénard, P.; Chahine, R.; Zong, Y.; Luo, M.; Yang, T. Neural Network Based Optimization for Cascade Filling Process of On-Board Hydrogen Tank. *Int. J. Hydrogen Energy* **2021**, *46*, 2936–2951. [CrossRef]

53. Yu, Y.; Lu, C.; Ye, S.; Hua, Z.; Gu, C. Optimization on Volume Ratio of Three-Stage Cascade Storage System in Hydrogen Refueling Stations. *Int. J. Hydrogen Energy* **2022**, *47*, 13430–13441. [CrossRef]

54. Luo, H.; Xiao, J.; Bénard, P.; Chahine, R.; Yang, T. Multi-Objective Optimization of Cascade Storage System in Hydrogen Refuelling Station for Minimum Cooling Energy and Maximum State of Charge. *Int. J. Hydrogen Energy* **2022**, *47*, 10963–10975. [CrossRef]

55. Caponi, R.; Ferrario, A.M.; Bocci, E.; Bødker, S.; del Zotto, L. Single-Tank Storage versus Multi-Tank Cascade System in Hydrogen Refueling Stations for Fuel Cell Buses. *Int. J. Hydrogen Energy* **2022**, *47*, 27633–27645. [CrossRef]

56. Xu, Z.; Dong, W.; Yang, K.; Zhao, Y.; He, G. Development of Efficient Hydrogen Refueling Station by Process Optimization and Control. *Int. J. Hydrogen Energy* **2022**, *47*, 23721–23730. [CrossRef]

57. Parks, G.; Boyd, R.; Cornish, J.; Remick, R. *Hydrogen Station Compression, Storage, and Dispensing Technical Status and Costs: Systems Integration*; National Renewable Energy Laboratory: Golden, CO, USA, 2014.

58. Tahan, M.-R. Recent Advances in Hydrogen Compressors for Use in Large-Scale Renewable Energy Integration. *Int. J. Hydrogen Energy* **2022**, *47*, 35275–35292. [CrossRef]

59. Genovese, M.; Fragiacomo, P. Parametric Technical-Economic Investigation of a Pressurized Hydrogen Electrolyzer Unit Coupled with a Storage Compression System. *Renew. Energy* **2021**, *180*, 502–515. [CrossRef]

60. Wang, T.; Jia, X.; Li, X.; Ren, S.; Peng, X. Thermal-Structural Coupled Analysis and Improvement of the Diaphragm Compressor Cylinder Head for a Hydrogen Refueling Station. *Int. J. Hydrogen Energy* **2020**, *45*, 809–821. [CrossRef]

61. Sdanghi, G.; Maranzana, G.; Celzard, A.; Fierro, V. Review of the Current Technologies and Performances of Hydrogen Compression for Stationary and Automotive Applications. *Renew. Sustain. Energy Rev.* **2019**, *102*, 150–170. [CrossRef]

62. Bhogilla, S.S.; Niyas, H. Design of a Hydrogen Compressor for Hydrogen Fueling Stations. *Int. J. Hydrogen Energy* **2019**, *44*, 29329–29337. [CrossRef]

63. Jia, X.; Chen, J.; Wu, H.; Peng, X. Study on the Diaphragm Fracture in a Diaphragm Compressor for a Hydrogen Refueling Station. *Int. J. Hydrogen Energy* **2016**, *41*, 6412–6421. [CrossRef]

64. Yu, W.; Dianbo, X.; Jianmei, F.; Xueyuan, P. Research on Sealing Performance and Self-Acting Valve Reliability in High-Pressure Oil-Free Hydrogen Compressors for Hydrogen Refueling Stations. *Int. J. Hydrogen Energy* **2010**, *35*, 8063–8070. [CrossRef]

65. Ligen, Y.; Vrubel, H.; Arlettaz, J.; Girault, H. Experimental Correlations and Integration of Gas Boosters in a Hydrogen Refueling Station. *Int. J. Hydrogen Energy* **2020**, *45*, 16663–16671. [CrossRef]

66. Pellegrini, M.; Guzzini, A.; Saccani, C. A Preliminary Assessment of the Potential of Low Percentage Green Hydrogen Blending in the Italian Natural Gas Network. *Energies* **2020**, *13*, 5570. [CrossRef]

67. Fragiacomo, P.; Genovese, M. Numerical Simulations of the Energy Performance of a PEM Water Electrolysis Based High-Pressure Hydrogen Refueling Station. *Int. J. Hydrogen Energy* **2020**, *45*, 27457–27470. [CrossRef]

68. Genovese, M.; Blekhman, D.; Dray, M.; Fragiacomo, P. Improving Chiller Performance and Energy Efficiency in Hydrogen Station Operation by Tuning the Auxiliary Cooling. *Int. J. Hydrogen Energy* **2022**, *47*, 2532–2546. [CrossRef]

69. Wang, Y.; Wang, S.; Decès-Petit, C. Evaluating the Measurement Uncertainty at Hydrogen Refueling Stations Using a Bayesian Non-Parametric Approach. *Int. J. Hydrogen Energy* **2022**, *47*, 7892–7901. [CrossRef]

70. De Huu, M.; Tschannen, M.; Bissig, H.; Stadelmann, P.; Büker, O.; MacDonald, M.; Maury, R.; Neuvonen, P.T.; Petter, H.T.; Rasmussen, K. Design of Gravimetric Primary Standards for Field-Testing of Hydrogen Refuelling Stations. *Flow Meas. Instrum.* **2020**, *73*, 101747. [CrossRef]

71. Büker, O.; Stolt, K.; de Huu, M.; MacDonald, M.; Maury, R. Investigations on Pressure Dependence of Coriolis Mass Flow Meters Used at Hydrogen Refueling Stations. *Flow Meas. Instrum.* **2020**, *76*, 101815. [CrossRef]

72. Haloua, F.; Bacquart, T.; Arrhenius, K.; Delobelle, B.; Ent, H. Metrology for Hydrogen Energy Applications: A Project to Address Normative Requirements. *Meas. Sci. Technol.* **2018**, *29*, 034001. [CrossRef]

73. Maury, R.; Auclercq, C.; Devilliers, C.; de Huu, M.; Büker, O.; MacDonald, M. Hydrogen Refuelling Station Calibration with a Traceable Gravimetric Standard. *Flow Meas. Instrum.* **2020**, *74*, 101743. [CrossRef]

74. Kim, W.; Shentsov, V.; Makarov, D.; Molkov, V. High Pressure Hydrogen Tank Rupture: Blast Wave and Fireball. In Proceedings of the 6th International Conference on Hydrogen Safety, Yokohama, Japan, 19–21 October 2015.

75. Makarov, D.; Shentsov, V.; Kuznetsov, M.; Molkov, V. Hydrogen Tank Rupture in Fire in the Open Atmosphere: Hazard Distance Defined by Fireball. *Hydrogen* **2021**, *2*, 134–146. [CrossRef]

76. Giannissi, S.G.; Tolias, I.C.; Melideo, D.; Baraldi, D.; Shentsov, V.; Makarov, D.; Molkov, V.; Venetsanos, A.G. On the CFD Modelling of Hydrogen Dispersion at Low-Reynolds Number Release in Closed Facility. *Int. J. Hydrogen Energy* **2021**, *46*, 29745–29761. [CrossRef]

77. Tolias, I.C.; Giannissi, S.G.; Venetsanos, A.G.; Keenan, J.; Shentsov, V.; Makarov, D.; Coldrick, S.; Kotchourko, A.; Ren, K.; Jedicke, O.; et al. Best Practice Guidelines in Numerical Simulations and CFD Benchmarking for Hydrogen Safety Applications. *Int. J. Hydrogen Energy* **2019**, *44*, 9050–9062. [CrossRef]

78. Handa, K.; Oshima, S.; Rembutsu, T. Precooling Temperature Relaxation Technology in Hydrogen Refueling for Fuel-Cell Vehicles. *Int. J. Hydrogen Energy* **2021**, *46*, 33511–33522. [CrossRef]

79. Genovese, M.; Blekhman, D.; Xie, C.; Dray, M.; Fragiacomo, P. Assuring Pulsation-Free Flow in a Directly Pressurized Fuel Delivery at a Retail Hydrogen Station. *Int. J. Hydrogen Energy* **2018**, *43*, 16623–16637. [CrossRef]

80. Genovese, M.; Blekhman, D.; Dray, M.; Fragiacomo, P. Hydrogen Losses in Fueling Station Operation. *J Clean Prod* **2020**, *248*, 119266. [CrossRef]

81. San Marchi, C.; Hecht, E.S.; Ekoto, I.W.; Groth, K.M.; LaFleur, C.; Somerday, B.P.; Mukundan, R.; Rockward, T.; Keller, J.; James, C.W. Overview of the DOE Hydrogen Safety, Codes and Standards Program, Part 3: Advances in Research and Development to Enhance the Scientific Basis for Hydrogen Regulations, Codes and Standards. *Int. J. Hydrogen Energy* **2017**, *42*, 7263–7274. [CrossRef]

82. Buttner, W.J.; Post, M.B.; Burgess, R.; Rivkin, C. An Overview of Hydrogen Safety Sensors and Requirements. *Int. J. Hydrogen Energy* **2011**, *36*, 2462–2470. [CrossRef]

83. Abohamzeh, E.; Salehi, F.; Sheikholeslami, M.; Abbassi, R.; Khan, F. Review of Hydrogen Safety during Storage, Transmission, and Applications Processes. *J. Loss Prev. Process Ind.* **2021**, *72*, 104569. [CrossRef]

84. Zou, Q.; Tian, Y.; Han, F. Prediction of State Property during Hydrogen Leaks from High-Pressure Hydrogen Storage Systems. *Int. J. Hydrogen Energy* **2019**, *44*, 22394–22404. [CrossRef]

85. Mathison, S.; Handa, K.; McGuire, T.; Brown, T.; Goldstein, T.; Johnston, M. Field Validation of the MC Default Fill Hydrogen Fueling Protocol. *SAE Int. J. Altern. Powertrains* **2015**, *4*, 130–144. [CrossRef]

86. Li, J.-Q.; Chen, Y.; Ma, Y.B.; Kwon, J.-T.; Xu, H.; Li, J.-C. A Study on the Joule-Thomson Effect of during Filling Hydrogen in High Pressure Tank. *Case Stud. Therm. Eng.* **2023**, *41*, 102678. [CrossRef]

87. Li, S.; Guo, J.; Lv, X.; Deng, T.; Cao, B.; Wang, J. Research on High-Pressure Hydrogen Pre-Cooling Based on CFD Technology in Fast Filling Process. *Processes* **2021**, *9*, 2208. [CrossRef]

88. Elgowainy, A.; Reddi, K. *Hydrogen Fueling Station Pre-Cooling Analysis*; 2016 DOE Hydrogen and Fuel Cells Program Annual Merit Review; Department of Energy (DOE): Dallas, TX, USA, 2016.

89. Elgowainy, A.; Reddi, K.; Lee, D.Y.; Rustagi, N.; Gupta, E. Techno-Economic and Thermodynamic Analysis of Pre-Cooling Systems at Gaseous Hydrogen Refueling Stations. *Int. J. Hydrogen Energy* **2017**, *42*, 29067–29079. [CrossRef]

90. Chen, J.; Gao, X.; Shao, S.; Hu, H.; Xie, J.; Li, N.; Gao, N. Numerical Investigation of the Vortex Tube Performance in Novel Precooling Methods in the Hydrogen Fueling Station. *Int. J. Hydrogen Energy* **2021**, *46*, 5548–5555. [CrossRef]

91. Piraino, F.; Blekhman, D.; Dray, M.; Fragiacomo, P. Empirically Verified Analysis of Dual Pre-Cooling System for Hydrogen Refuelling Station. *Renew Energy* **2021**, *63*, 1612–1625. [CrossRef]

92. Xiao, R.; Tian, G.; Hou, Y.; Chen, S.; Cheng, C.; Chen, L. Effects of Cooling-Recovery Venting on the Performance of Cryo-Compressed Hydrogen Storage for Automotive Applications. *Appl. Energy* **2020**, *269*, 115143. [CrossRef]

93. Genovese, M.; Blekhman, D.; Dray, M.; Fragiacomo, P. Hydrogen Station in Situ Back-to-Back Fueling Data for Design and Modeling. *J. Clean. Prod.* **2021**, *329*, 129737. [CrossRef]

94. Liu, J.; Ma, H.; Zheng, S.; Zhang, Z.; Zheng, J.; Zhao, Y. Numerical investigation on temperature-rise of on-bus gaseous hydrogen storage cylinder with different thickness of liner and wrapping material. *Int. J. Hydrogen Energy* **2021**, *46*, 20607–20620. [CrossRef]

95. Oh, S.J.; Yoon, J.H.; Jeon, K.S.; Choi, J. A Numerical Study on Characteristics of Heat Transfer in Hydrogen Filling Storage Vessel by Charging Conditions. *Int. J. Hydrogen Energy* **2022**, *47*, 25679–25695. [CrossRef]

96. Li, M.; Bai, Y.; Zhang, C.; Song, Y.; Jiang, S.; Grouset, D.; Zhang, M. Review on the Research of Hydrogen Storage System Fast Refueling in Fuel Cell Vehicle. *Int. J. Hydrogen Energy* **2019**, *44*, 10677–10693. [CrossRef]

97. Guo, J.; Yang, J.; Zhao, Y.; Pan, X.; Zhang, L.; Zhao, L.; Zheng, J. Investigations on Temperature Variation within a Type III Cylinder during the Hydrogen Gas Cycling Test. *Int. J. Hydrogen Energy* **2014**, *39*, 13926–13934. [CrossRef]
98. Simonovski, I.; Baraldi, D.; Melideo, D.; Acosta-Iborra, B. Thermal Simulations of a Hydrogen Storage Tank during Fast Filling. *Int. J. Hydrogen Energy* **2015**, *40*, 12560–12571. [CrossRef]
99. Liu, Y.-L.; Zhao, Y.-Z.; Zhao, L.; Li, X.; Chen, H.; Zhang, L.-F.; Zhao, H.; Sheng, R.-H.; Xie, T.; Hu, D.-H.; et al. Experimental Studies on Temperature Rise within a Hydrogen Cylinder during Refueling. *Int. J. Hydrogen Energy* **2010**, *35*, 2627–2632. [CrossRef]
100. Dicken, C.J.B.; Mérida, W. Measured Effects of Filling Time and Initial Mass on the Temperature Distribution within a Hydrogen Cylinder during Refuelling. *J. Power Sources* **2007**, *165*, 324–336. [CrossRef]
101. Kim, S.C.; Lee, S.H.; Yoon, K.B. Thermal Characteristics during Hydrogen Fueling Process of Type IV Cylinder. *Int. J. Hydrogen Energy* **2010**, *35*, 6830–6835. [CrossRef]
102. Zheng, J.; Ye, J.; Yang, J.; Tang, P.; Zhao, L.; Kern, M. An Optimized Control Method for a High Utilization Ratio and Fast Filling Speed in Hydrogen Refueling Stations. *Int. J. Hydrogen Energy* **2010**, *35*, 3011–3017. [CrossRef]
103. Zhao, L.; Liu, Y.; Yang, J.; Zhao, Y.; Zheng, J.; Bie, H.; Liu, X. Numerical Simulation of Temperature Rise within Hydrogen Vehicle Cylinder during Refueling. *Int. J. Hydrogen Energy* **2010**, *35*, 8092–8100. [CrossRef]
104. Li, Q.; Zhou, J.; Chang, Q.; Xing, W. Effects of Geometry and Inconstant Mass Flow Rate on Temperatures within a Pressurized Hydrogen Cylinder during Refueling. *Int. J. Hydrogen Energy* **2012**, *37*, 6043–6052. [CrossRef]
105. Olmos, F.; Manousiouthakis, V.I. Gas Tank Fill-up in Globally Minimum Time: Theory and Application to Hydrogen. *Int. J. Hydrogen Energy* **2014**, *39*, 12138–12157. [CrossRef]
106. Zheng, J.; Guo, J.; Yang, J.; Zhao, Y.; Zhao, L.; Pan, X.; Ma, J.; Zhang, L. Experimental and Numerical Study on Temperature Rise within a 70 MPa Type III Cylinder during Fast Refueling. *Int. J. Hydrogen Energy* **2013**, *38*, 10956–10962. [CrossRef]
107. Rothuizen, E.; Mérida, W.; Rokni, M.; Wistoft-Ibsen, M. Optimization of Hydrogen Vehicle Refueling via Dynamic Simulation. *Int. J. Hydrogen Energy* **2013**, *38*, 4221–4231. [CrossRef]
108. Suryan, A.; Kim, H.D.; Setoguchi, T. Comparative Study of Turbulence Models Performance for Refueling of Compressed Hydrogen Tanks. *Int. J. Hydrogen Energy* **2013**, *38*, 9562–9569. [CrossRef]
109. Ruffio, E.; Saury, D.; Petit, D. Thermodynamic Analysis of Hydrogen Tank Filling. Effects of Heat Losses and Filling Rate Optimization. *Int. J. Hydrogen Energy* **2014**, *39*, 12701–12714. [CrossRef]
110. Wang, G.; Zhou, J.; Hu, S.; Dong, S.; Wei, P. Investigations of Filling Mass with the Dependence of Heat Transfer during Fast Filling of Hydrogen Cylinders. *Int. J. Hydrogen Energy* **2014**, *39*, 4380–4388. [CrossRef]
111. Ortiz Cebolla, R.; Acosta, B.; de Miguel, N.; Moretto, P. Effect of Precooled Inlet Gas Temperature and Mass Flow Rate on Final State of Charge during Hydrogen Vehicle Refueling. *Int. J. Hydrogen Energy* **2015**, *40*, 4698–4706. [CrossRef]
112. Bourgeois, T.; Ammouri, F.; Weber, M.; Knapik, C. Evaluating the Temperature inside a Tank during a Filling with Highly-Pressurized Gas. *Int. J. Hydrogen Energy* **2015**, *40*, 11748–11755. [CrossRef]
113. De Miguel, N.; Acosta, B.; Baraldi, D.; Melideo, R.; Ortiz Cebolla, R.; Moretto, P. The Role of Initial Tank Temperature on Refuelling of On-Board Hydrogen Tanks. *Int. J. Hydrogen Energy* **2016**, *41*, 8606–8615. [CrossRef]
114. de Miguel, N.; Acosta, B.; Moretto, P.; Ortiz Cebolla, R. Influence of the Gas Injector Configuration on the Temperature Evolution during Refueling of On-Board Hydrogen Tanks. *Int. J. Hydrogen Energy* **2016**, *41*, 19447–19454. [CrossRef]
115. Xiao, J.; Bénard, P.; Chahine, R. Charge-Discharge Cycle Thermodynamics for Compression Hydrogen Storage System. *Int. J. Hydrogen Energy* **2016**, *41*, 5531–5539. [CrossRef]
116. Xiao, J.; Wang, X.; Bénard, P.; Chahine, R. Determining Hydrogen Pre-Cooling Temperature from Refueling Parameters. *Int. J. Hydrogen Energy* **2016**, *41*, 16316–16321. [CrossRef]
117. Cheng, J.; Xiao, J.; Bénard, P.; Chahine, R. Estimation of Final Hydrogen Temperatures During Refueling 35 MPa and 70 MPa Tanks. *Energy Procedia* **2017**, *105*, 1363–1369. [CrossRef]
118. Wang, X.; Xiao, J.; Bénard, P.; Chahine, R. Final Hydrogen Mass Determined from Refueling Parameters. *Energy Procedia* **2017**, *105*, 1370–1375. [CrossRef]
119. Xiao, J.; Bénard, P.; Chahine, R. Estimation of Final Hydrogen Temperature from Refueling Parameters. *Int. J. Hydrogen Energy* **2017**, *42*, 7521–7528. [CrossRef]
120. Bourgeois, T.; Brachmann, T.; Barth, F.; Ammouri, F.; Baraldi, D.; Melideo, D.; Acosta-Iborra, B.; Zaepffel, D.; Saury, D.; Lemonnier, D. Optimization of Hydrogen Vehicle Refuelling Requirements. *Int. J. Hydrogen Energy* **2017**, *42*, 13789–13809. [CrossRef]
121. Kuroki, T.; Sakoda, N.; Shinzato, K.; Monde, M.; Takata, Y. Dynamic Simulation for Optimal Hydrogen Refueling Method to Fuel Cell Vehicle Tanks. *Int. J. Hydrogen Energy* **2018**, *43*, 5714–5721. [CrossRef]
122. Kuroki, T.; Sakoda, N.; Shinzato, K.; Monde, M.; Takata, Y. Prediction of Transient Temperature of Hydrogen Flowing from Pre-Cooler of Refueling Station to Inlet of Vehicle Tank. *Int. J. Hydrogen Energy* **2018**, *43*, 1846–1854. [CrossRef]
123. Xiao, J.; Cheng, J.; Wang, X.; Bénard, P.; Chahine, R. Final Hydrogen Temperature and Mass Estimated from Refueling Parameters. *Int. J. Hydrogen Energy* **2018**, *43*, 22409–22418. [CrossRef]
124. Xiao, J.; Wang, X.; Zhou, X.; Bénard, P.; Chahine, R. A Dual Zone Thermodynamic Model for Refueling Hydrogen Vehicles. *Int. J. Hydrogen Energy* **2019**, *44*, 8780–8790. [CrossRef]
125. Melideo, D.; Baraldi, D.; de Miguel Echevarria, N.; Acosta Iborra, B. Effects of Some Key-Parameters on the Thermal Stratification in Hydrogen Tanks during the Filling Process. *Int. J. Hydrogen Energy* **2019**, *44*, 13569–13582. [CrossRef]

126. Sapre, S.; Pareek, K.; Rohan, R.; Singh, P.K. H2 Refueling Assessment of Composite Storage Tank for Fuel Cell Vehicle. *Int. J. Hydrogen Energy* **2019**, *44*, 23699–23707. [CrossRef]
127. Zhou, X.; Yang, T.; Xiao, J.; Bénard, P.; Chahine, R. Estimation of Filling Time for Compressed Hydrogen Refueling. *Energy Procedia* **2019**, *158*, 1897–1903. [CrossRef]
128. Wang, L.; Ye, F.; Xiao, J.; Bénard, P.; Chahine, R. Heat Transfer Analysis for Fast Filling of On-Board Hydrogen Tank. *Energy Procedia* **2019**, *158*, 1910–1916. [CrossRef]
129. Liu, J.; Zheng, S.; Zhang, Z.; Zheng, J.; Zhao, Y. Numerical Study on the Fast Filling of On-Bus Gaseous Hydrogen Storage Cylinder. *Int. J. Hydrogen Energy* **2020**, *45*, 9241–9251. [CrossRef]
130. Jiang, Y.; Wei, S.T.; Xu, P. Influences of Filling Process on the Thermal-Mechanical Behavior of Composite Overwrapped Pressure Vessel for Hydrogen. *Int. J. Hydrogen Energy* **2020**, *45*, 23093–23102. [CrossRef]
131. Wang, Y.; Decès-Petit, C. Predicting Fueling Process on Hydrogen Refueling Stations Using Multi-Task Machine Learning. *Int. J. Hydrogen Energy* **2020**, *45*, 32743–32752. [CrossRef]
132. Deng, S.; Xiao, J.; Bénard, P.; Chahine, R. Determining Correlations between Final Hydrogen Temperature and Refueling Parameters from Experimental and Numerical Data. *Int. J. Hydrogen Energy* **2020**, *45*, 20525–20534. [CrossRef]
133. Wen, C.; Rogie, B.; Kærn, M.R.; Rothuizen, E. A First Study of the Potential of Integrating an Ejector in Hydrogen Fuelling Stations for Fuelling High Pressure Hydrogen Vehicles. *Appl. Energy* **2020**, *260*, 113958. [CrossRef]
134. Rothuizen, E.; Elmegaard, B.; Rokni, M. Dynamic Simulation of the Effect of Vehicle-Side Pressure Loss of Hydrogen Fueling Process. *Int. J. Hydrogen Energy* **2020**, *45*, 9025–9038. [CrossRef]
135. Sapre, S.; Vyas, M.; Pareek, K. Impact of Refueling Parameters on Storage Density of Compressed Hydrogen Storage Tank. *Int. J. Hydrogen Energy* **2021**, *46*, 16685–16692. [CrossRef]
136. Caponi, R.; Monforti Ferrario, A.; Bocci, E.; Valenti, G.; della Pietra, M. Thermodynamic Modeling of Hydrogen Refueling for Heavy-Duty Fuel Cell Buses and Comparison with Aggregated Real Data. *Int. J. Hydrogen Energy* **2021**, *46*, 18630–18643. [CrossRef]
137. Kuroki, T.; Nagasawa, K.; Peters, M.; Leighton, D.; Kurtz, J.; Sakoda, N.; Monde, M.; Takata, Y. Thermodynamic Modeling of Hydrogen Fueling Process from High-Pressure Storage Tank to Vehicle Tank. *Int. J. Hydrogen Energy* **2021**, *46*, 22004–22017. [CrossRef]
138. Li, H.; Lyu, Z.; Liu, Y.; Han, M.; Li, H. The Effects of Infill on Hydrogen Tank Temperature Distribution during Fast Fill. *Int. J. Hydrogen Energy* **2021**, *46*, 10396–10410. [CrossRef]
139. Bai, Y.; Zhang, C.; Duan, H.; Jiang, S.; Zhou, Z.; Grouset, D.; Zhang, M.; Ye, X. Modeling and Optimal Control of Fast Filling Process of Hydrogen to Fuel Cell Vehicle. *J. Energy Storage* **2021**, *35*, 102306. [CrossRef]
140. Wu, X.; Liu, J.; Shao, J.; Deng, G. Fast Filling Strategy of Type III On-Board Hydrogen Tank Based on Time-Delayed Method. *Int. J. Hydrogen Energy* **2021**, *46*, 29288–29296. [CrossRef]
141. Wang, Y.; Wang, S.; Decès-Petit, C. Less Is More: Robust Prediction for Fueling Processes on Hydrogen Refueling Stations. *Int. J. Hydrogen Energy* **2022**, *47*, 28993–29005. [CrossRef]
142. Kawatsu, K.; Suzuki, T.; Shiota, K.; Izato, Y.; Komori, M.; Sato, K.; Takai, Y.; Ninomiya, T.; Miyake, A. Dynamic Physical Model of Japanese Hydrogen Refueling Stations for Quantitative Trade-off Study between Benefit and Risk. *Int. J. Hydrogen Energy* **2022**. [CrossRef]
143. Chen, J.; Xiao, L.; Wu, Y.; Gao, X.; Chen, H.; Xie, J.; Shao, S. Dynamic Simulation of the Potential of Integrating a Turbo-Expander in a Hydrogen Refueling Station. *Appl. Therm. Eng.* **2022**, *202*, 117889. [CrossRef]
144. Park, B.H.; Chae, C.K. Development of Correlation Equations on Hydrogen Properties for Hydrogen Refueling Process by Machine Learning Approach. *Int. J. Hydrogen Energy* **2022**, *47*, 4185–4195. [CrossRef]
145. Li, J.-Q.; Li, J.-C.L.; Park, K.; Kwon, J.-T. Investigation on the Changes of Pressure and Temperature in High Pressure Filling of Hydrogen Storage Tank. *Case Stud. Therm. Eng.* **2022**, *37*, 102143. [CrossRef]
146. Deng, S.; Li, F.; Luo, H.; Yang, T.; Ye, F.; Chahine, R.; Xiao, J. Lumped Parameter Modeling of SAE J2601 Hydrogen Fueling Tests. *Sustainability* **2023**, *15*, 1448. [CrossRef]
147. Genovese, M.; Cigolotti, V.; Jannelli, E.; Fragiacomo, P. Current Standards and Configurations for the Permitting and Operation of Hydrogen Refueling Stations. *Int. J. Hydrogen Energy* **2023**. [CrossRef]
148. *Society of Automotive Engineers (SAE) SAE J2601(2016): Fueling Protocols for Light Duty Gaseous Hydrogen Surface Vehicles*; SAE International Headquarters 400 Commonwealth Drive: Warrendale, PA, USA, 2016.
149. Maus, S.; Hapke, J.; Ranong, C.N.; Wüchner, E.; Friedlmeier, G.; Wenger, D. Filling Procedure for Vehicles with Compressed Hydrogen Tanks. *Int. J. Hydrogen Energy* **2008**, *33*, 4612–4621. [CrossRef]
150. Wang, X.; Fu, J.; Liu, Z.; Liu, J. Review of Researches on Important Components of Hydrogen Supply Systems and Rapid Hydrogen Refueling Processes. *Int. J. Hydrogen Energy* **2023**, *48*, 1904–1929. [CrossRef]
151. Ku, A.Y.; Reddi, K.; Elgowainy, A.; McRobie, J.; Li, J. Liquid Pump-Enabled Hydrogen Refueling System for Medium and Heavy Duty Fuel Cell Vehicles: Station Design and Technoeconomic Assessment. *Int. J. Hydrogen Energy* **2022**, *47*, 25486–25498. [CrossRef]
152. Apostolou, D. Refuelling Scenarios of a Light Urban Fuel Cell Vehicle with Metal Hydride Hydrogen Storage. Comparison with Compressed Hydrogen Storage Counterpart. *Int. J. Hydrogen Energy* **2021**, *46*, 39509–39522. [CrossRef]

153. Li, J.; Youn, E.; Ramteke, A.; McRobie, J.; Hansen, E.; Hall, C.; Kratschmar, K.; Prakash, A.; Conrad, K.; Ku, A.Y. Liquid Pump-Enabled Hydrogen Refueling System for Heavy Duty Fuel Cell Vehicles: Fuel Cell Bus Refueling Demonstration at Stark Area Regional Transit Authority (SARTA). *Int. J. Hydrogen Energy* **2021**, *46*, 38575–38587. [CrossRef]
154. PRHYDE Project on Heavy-Duty Hydrogen Refueling Protocol. *Fuel Cells Bulletin* **2020**, *2020*, 8–9. [CrossRef]
155. LaChance, J.; Tchouvelev, A.; Ohi, J. Risk-Informed Process and Tools for Permitting Hydrogen Fueling Stations. *Int. J. Hydrogen Energy* **2009**, *34*, 5855–5861. [CrossRef]
156. Böhm, M.; Fernández Del Rey, A.; Pagenkopf, J.; Varela, M.; Herwartz-Polster, S.; Nieto Calderón, B. Review and Comparison of Worldwide Hydrogen Activities in the Rail Sector with Special Focus on On-Board Storage and Refueling Technologies. *Int. J. Hydrogen Energy* **2022**, *47*, 38003–38017. [CrossRef]
157. Petitpas, G.; Aceves, S.M.; Gupta, N. Vehicle Refueling with Liquid Hydrogen Thermal Compression. *Int. J. Hydrogen Energy* **2012**, *37*, 11448–11457. [CrossRef]
158. Petitpas, G.; Moreno-Blanco, J.; Espinosa-Loza, F.; Aceves, S.M. Rapid High Density Cryogenic Pressure Vessel Filling to 345 Bar with a Liquid Hydrogen Pump. *Int. J. Hydrogen Energy* **2018**, *43*, 19547–19558. [CrossRef]
159. Charolais, A.; Ammouri, F.; Vyazmina, E.; Werlen, É.; Harris, A. Safety Watchdog for Universally Safe Gaseous High Pressure Hydrogen Fillings. *Int. J. Hydrogen Energy* **2021**, *46*, 16019–16029. [CrossRef]
160. Striednig, M.; Brandstätter, S.; Sartory, M.; Klell, M. Thermodynamic Real Gas Analysis of a Tank Filling Process. *Int. J. Hydrogen Energy* **2014**, *39*, 8495–8509. [CrossRef]
161. Moreno-Blanco, J.; Camacho, G.; Valladares, F.; Aceves, S.M. The Cold High-Pressure Approach to Hydrogen Delivery. *Int. J. Hydrogen Energy* **2020**, *45*, 27369–27380. [CrossRef]
162. Petitpas, G.; Aceves, S.M. Liquid Hydrogen Pump Performance and Durability Testing through Repeated Cryogenic Vessel Filling to 700 Bar. *Int. J. Hydrogen Energy* **2018**, *43*, 18403–18420. [CrossRef]